

Solid state thermochromic materials

Pragna Kiri^a, Geoff Hyett^b, Russell Binions^{a*}

^aDepartment of Chemistry, University College London, Christopher Ingold Laboratories, 20 Gordon Street, London, WC1H 0AJ, United Kingdom

^bSchool of Chemistry, University of Leeds, Leeds, LS2 9JT, United Kingdom

*Corresponding author. Tel.: (+44) 20 76791460; E-mail: R.Binions@ucl.ac.uk

Received: 03 Aug 2010, Revised: 05 Aug 2010 and Accepted: 07 Aug 2010

ABSTRACT

Solid-state thermochromic materials undergo semiconductor to metal transitions at a 'critical temperature', T_c . This review begins by describing the phenomenon of thermochromism, whereby the optical properties of a material change reversibly as a result of a change in temperature. The various different types of thermochromism will be introduced with a focus on the thermochromism exhibited by solid-state materials. The fundamental chemical principles that describe the electronic structure and properties of solids, and the chronological developments in the theory behind the thermochromic transitions (such as, the effects of electron-electron interactions and structural phase changes due to lattice distortions) that led to the discovery of the semiconductor-to-metal transition, are presented. An extensive discussion of vanadium and titanium oxides is presented with a particular focus on vanadium (IV) oxide since its transition temperature is closest to room temperature. Observations and current understanding of the nature of the semiconductor-to-metal transition exhibited by these materials is detailed. The possibility of fine-tuning the transition temperature by introducing various dopants into the vanadium (IV) oxide lattice is examined and the effects of dopant charge and size is examined. Solid-state thermochromic materials may be exploited in areas such as microelectronics, data storage, or intelligent architectural glazing, thus are required to be synthesised as thin films for use in such applications. The numerous synthetic techniques (PVD, sol-gel method, PLD, CVD, APCVD and AACVD), for making metal oxide thermochromic thin films are described in reference to the production of vanadium (IV) oxide and compared. Finally rare earth nickelates exhibiting thermochromism are described. Copyright © 2010 VBRI press.

Keywords: Thermochromic materials; semiconductor; solid-state; thin films.



Pragna Kiri is a final year undergraduate student based in the department of Chemistry at UCL. Her research is centered on the synthesis of fluorine doped vanadium dioxide thin films using aerosol assisted chemical vapour deposition techniques for use in intelligent architectural glazing.

functional thin films with Prof Ivan Parkin at UCL until 2009 when he took up the Ramsay Fellowship.



Russell Binions is a Royal Society Dorothy Hodgkin research fellow based in the department of chemistry, University College London (UCL), UK. His research interests include the synthesis of thin films of thermochromic materials, the deposition of multifunctional nanocomposite thin films, the application of electric fields in chemical vapour deposition reactions and metal oxide gas sensors for application in breath analysis and environmental monitoring. He completed his postgraduate studies at UCL and has previously held postdoctoral positions at UCL with Prof. Ivan Parkin researching into vanadium dioxide thin films for glazing applications and the use of zeolites in modifying gas sensor response.



Geoff Hyett is a lecturer in inorganic-materials chemistry at the University of Leeds. His research interests include the synthesis of thin films, water-splitting photocatalysis and novel mixed-anion solid-state compounds. His previous appointments include a Ramsay Research Fellowship held at UCL, and a sessional lectureship at Birkbeck, University of London. He carried out his post graduate studies at the University of Oxford, and conducted postdoctoral research into

Contents

1. Introduction and chemical principles
 - 1.1. What is a thermochromic material?
 - 1.2. Semiconductor-to-metal transitions
2. Thermochromic transition metal oxides
 - 2.1. V_2O_3
 - 2.2. V_2O_5
 - 2.3. VO_2
 - 2.4. V_6O_{13}
 - 2.5. Ti_nO_{2n+1} magnéli phases
3. Effects of dopants
4. Synthetic techniques
 - 4.1. Physical vapour deposition
 - 4.2. Pulsed laser deposition
 - 4.3. Sol-gel synthesis
 - 4.4. Chemical vapour deposition
 - 4.4.1. Atmospheric pressure chemical vapour deposition
 - 4.4.2. Aerosol assisted chemical vapour deposition
 - 4.5. Comparison of production methods
5. Applications of thermochromic thin films
6. Thermochromic lanthanide compounds
 - 6.1 Rare earth nickelates
7. Conclusion
8. Acknowledgments
9. Abbreviations
10. References

1. Introduction and chemical principles

1.1. What is a thermochromic material?

“Chromeogenic” materials are those that exhibit changes in their optical properties due to some external stimulus. The most common of these are photochromic, thermochromic and electrochromic materials, where the stimuli are irradiation by light (photons), change in temperature, and an applied electric field, respectively. Thus, a thermochromic material changes colour upon reaching a characteristic ‘transition temperature’. Broadly speaking, thermochromism is the temperature-dependant changes in the optical properties of a material. Typically, the thermochromic effect occurs over a range of temperatures, which is observed as a gradual colour change, i.e. continuous thermochromism. Discontinuous thermochromism involves a structural phase change at the transition temperature. This phase change can be first- or second-order in nature, and may be reversible or irreversible, as governed by the thermodynamics of the system [1]. Thermochromism offers potential for technological applications, for example, in thermometers (fever indicators, gadgets, design applications, etc.), temperature sensors for safety, laser marking, or warning signals. As well as inorganic oxides, many different compounds, for instance, liquid crystals [2], conjugated oligomers [3], leuco dyes [4], are all commonly known to exhibit the ability to reversibly change colour with temperature. However, thermochromic dyes are usually based on organic compounds, which show irreversible colour changes on heating.

1.2. Semiconductor-to-metal transitions

The non-interacting, free-electron model of the electronic structure of solids by Wilson and Fowler in 1931 [5, 6] successfully describes the distinction between metals and non-metals at absolute zero. It was acknowledged that insulators with small energy gaps between the highest filled band and lowest empty band would be semiconductors upon thermal excitation of the electrons.

However, the findings of transition-metal oxides existing as insulators by de Boer and Verway (1937) [7] despite exhibiting partially filled $3d$ bands, confirms the inadequacy of simple band theory due to the neglect of electron repulsion. Following this finding, Peierls (1937) [8] then pointed out the importance of the electron-electron correlation, stating that strong Coulombic repulsion between the electrons could be the origin of the insulating behaviour, where at low temperatures, the electrons are in their “proper” positions. Thermal excitation is required to cross the potential barrier for the movement of electrons into the metallic, conducting state. Wigner in 1938 [9] introduced electron-electron interactions and suggested that a free electron gas should ‘crystallize’ in a non-conducting state. Mott confirmed this in 1949 [10] and suggested that electrons become localized by the Coulombic repulsion between two $3d$ electrons of opposite spin on the same ion. He described a semiconductor-to-metal transition by imagining a crystalline array of one-electron atoms with a variable lattice constant, b . At large values of b the material would be insulating, and at small values it would be metallic. Thus, b has a critical value, b_0 , at which a transition occurs. If b is larger than b_0 , an activation energy is required to form a pair of carriers. As b becomes smaller, the activation energy decreases. This drop in activation energy is a discontinuous transition (Fig. 1), because an electron and positive hole can form a pair owing to their Coulombic attraction and mutual potential energy. In 1961, Mott proposed further that the transition between an insulating ground state and the conducting ground state, using a band approach, occurs sharply at b_0 for each material. This is known as the “Mott transition” [11, 12].

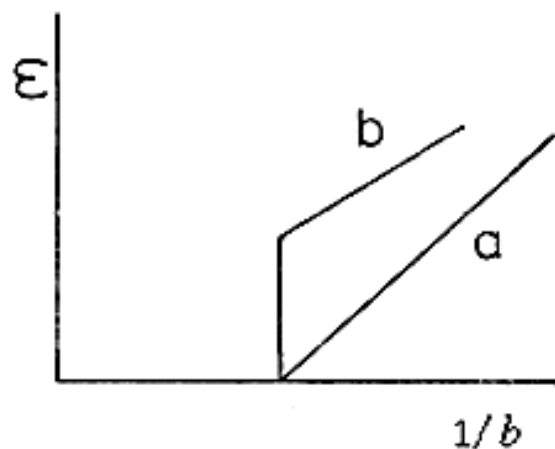


Fig.1. The change in activation energy (ϵ) versus reciprocal lattice constant ($1/b$). a- shows a continuous change, where as b- shows a discontinuous change.

Mott's hypothesis has come to be known as the short-range, one band model. Hubbard [13] developed the theory in 1963, where interionic, long-range Coulombic interactions are also neglected and are only important when the electrons are on the same atom. Hence, by quantitatively treating the Mott transition, he found that at a critical ratio of the band width to the intraionic Coulomb energy, the energy gap due to electronic correlations in the partially filled narrow bands had reduced to zero and thus an insulator-to-metal transition occurred.

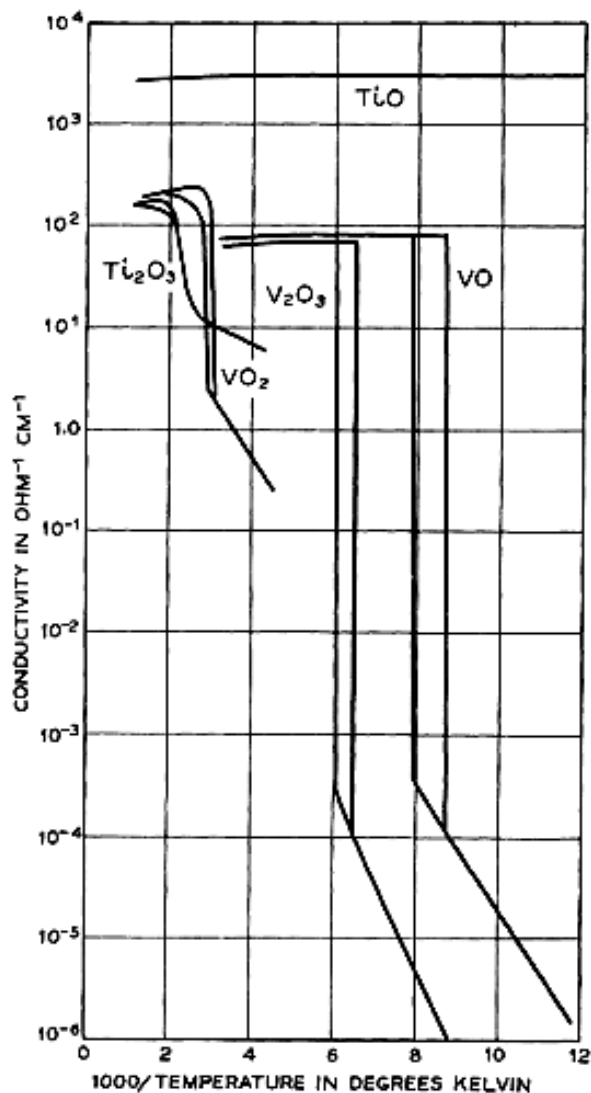


Fig. 2. Taken from [17] Shows a plot of conductivity versus reciprocal temperature for the lower oxides of vanadium and titanium.

A different approach using a two band model was proposed by Slater in 1951 [14]. He found that the insulating properties of the ground state in antiferromagnetic transition-metal compounds with large values of b can be explained by supposing the d -band splits at the Néel temperature, as observed in NiS, which allows all bands to be full or empty [15]. Therefore, it is antiferromagnetic ordering that leads to the insulating nature of the ground state, but it is not clear why the insulating property does not disappear above the Néel

temperature. When the two bands are present (lower and upper Hubbard bands), there is a band-crossing transition from antiferromagnetic metal to antiferromagnetic insulator. A related transition from the antiferromagnetic metal to the 'normal' metal was first observed in vanadium oxides by Brinkman and Rice in 1970 [16].

Transition-metal oxides such as Ti_2O_3 , V_2O_3 , VO_2 , and VO are all semi-conducting at low temperatures and show a transition into a metallic state at the Néel temperature. The electrical properties of these oxides were thoroughly studied using thermo-conductive studies by Morin in 1959 [17]. One of the complications in studying these materials is the difficulty in growing pure, stoichiometric single crystals. He found that all lower oxides of titanium and vanadium exhibit this behaviour (Fig. 2) except for TiO , which is metallic over the entire temperature range.

Morin attempted to explain the discontinuities in conductivities of the oxides by adapting Slater's two-band model. The transition was originally named a metal-to-insulator transition due to the changes in conductive properties of the materials, but other properties of these materials soon became apparent and it was therefore re-labelled as a metal-to-semiconductor transition [18, 19]. For this reason, the semiconductor-to-metal transition due to the $3d$ band splitting (arising from antiferromagnetism) would be expected at the Néel temperature. The Slater-Morin theory has never been quantitatively applied to the oxides of vanadium and titanium, which is only one of the theory's limitations. Another problem with the theory is that antiferromagnetism had only been confirmed to exist in Ti_2O_3 [20], which was found to be extremely small. Additionally, the structure of the degenerate $3d$ bands and the antiferromagnetic splitting in attempt to explain how TiO , VO or VO could be insulating at 0 K, could not be modelled.

Not all semiconductor-to-metal transitions are the result of electron-electron interactions. The nature of the transition is not entirely inexplicable in the theory of non-interacting electrons, since changes in crystal structure may also lead to the formation of a band gap. Their optical properties also showed large decreases in transmittance and increases in reflectance on passing through the transition temperature. In 1967-8, Adler and Brooks [21, 22] found that transition-metal oxides can be insulators, semiconductors, metals or undergo metal to non-metal transitions. They also discovered that band theory can be adapted to explain most of the materials that exhibit metal to non-metal transitions. It was found that a lattice distortion occurs at the transition point, causing an energy gap between occupied and empty states. As the temperature is raised, the energy gap between the valence and conduction bands decreases linearly with the number of electrons excited across the gap. This results show rapid disappearance of the distortion, and hence the band gap. The material is then metallic. The phase transition can be first- or second-order in nature, which depends on the magnitude of the relative change in the gap with the number of excited carriers [21]. The 'order' of a phase transition is classified by considering the thermodynamic potential, (for example the Gibbs free energy surface, G) and its derivatives at the transition. During a phase transition, the free energy of the solid remains continuous, but

thermodynamic quantities, such as entropy, volume and heat capacity exhibit discontinuous change. If the first derivative of G , with respect to a thermodynamic variable, is discontinuous the transition is called 'first-order'. If the first derivatives are continuous, but second derivatives (at least one) exhibit discontinuities, the transition is classed at 'second-order', for instance, a critical point on a phase diagram. In a first-order transition where the $G(p,T)$ surfaces of the initial state and final state intersect sharply, the entropy and the volume show singular behaviour, thus there is a latent heat. Alternatively, in second-order transitions, the heat capacity, compressibility, or thermal expansivity shows singular behaviour, and so do not involve a latent heat, since the change in entropy is continuous [23]. Landau introduced the concept of an order parameter, ξ , which is a measure of the order that results from a phase transition. In a first-order transition, the change in ξ is discontinuous, but in a second-order transition, i.e., the change of state is continuous, therefore the change in ξ is also continuous. Landau postulated that in a second-order (or structural) phase transition, G is not only a function of p and T but also of ξ . He consequently expanded G as a series of powers of ξ around the transition point, where the order parameter is seen to disappear at the critical temperature, T_c . Furthermore, Landau regarded the simultaneous symmetry changes from a phase of high symmetry to low symmetry during phase transitions, have an associated order parameter.

Adler and Brooks postulated two models for the likely mechanism of the semiconductor-to-metal transition. One suggesting that the band gap results from the splitting of the first Brillouin zone [24] by an antiferromagnetic exchange interaction, giving a second-order transition. In the Linear Combination of Atomic Orbitals (LCAO) approach to band theory, the first Brillouin zone gives the range of wave vectors, k , that are necessary in order to generate all possible, distinguishable Bloch [25] sums of atomic orbitals. Periodic arrangements of atoms must satisfy the Bloch wave function **equation (1)**, constructed from the overlapping of atomic orbitals.

$$\Psi(x) = \exp(ikx) u(x) \quad \text{----- (1)}$$

Where, $u(x)$ is any function that is periodic and must not be altered when moving from one atom to another in a lattice. The $\exp(ikx)$ term adjusts the amplitude of the wave. All functions have a wave-like form, thus a crystal orbital has a wavelength determined by quantum number, k , also known as the wave number (or vector), where wavelength, $\lambda = 2\pi/k$. Since properties such as conductivity depend on the motion of electron in crystals, the Bloch function equation is also applied in the free-electron theory, where k is proportional to the momentum of an electron.

The other model suggests the band gap results from a crystalline-structure distortion, in terms of the pairing ions in a one dimensional crystal, to lower symmetry. This gives a first-order transition. The band gap formed must decrease with thermal excitation, and at a given temperature a transition to a metallic state occurs. Generally, either first- or second-order transitions are possible for

antiferromagnets and distorted crystals, although the former is more likely to undergo a second-order transition than a distorted crystal. The findings of Alder and Brooks' study helped to explain the results of Morin's study on the conductivities of titanium and vanadium oxides by describing the following: when the free energy of a metallic state falls below the local minimum for the semiconducting state, a first-order transition will result. However, the continual existence of the local minimum up to the second-order transition temperature could lead to a metastable state. Experimentally, this local minimum of free energy would appear as a hysteresis when the material is heated in the semiconducting state. The hysteresis would not occur when the transition is second-order. Hence, the order of the transition can clearly be determined directly from Morin's electrical conductivity data, indicating that V_2O_3 , VO and VO_2 undergo first-order transitions, while Ti_2O_3 exhibits a second-order transition.

2. Thermochromic transition metal oxides

Transition-metal oxides are the most studied solid-state thermochromic materials, since the discovery of the phase transitions that occur at a critical temperature, T_c , where an abrupt change in optical and electronic properties is observed, making them ideal subjects for an investigation of non-metallic and metallic states. Adler (1968) initially found that the main obstacle when studying these materials was the difficulty in growing pure, stoichiometric single crystals, and therefore found that the original electrical measurements obtained were not linked to the intrinsic properties of the materials but due to the large concentrations of lattice defects and impurities. Owing to the improvements and developments of crystal growth techniques and equipment at the time of investigation, pure stoichiometric crystalline transition metal oxides (and sulfides) were classified as metals or semiconductors and insulators that can undergo semiconductor-to-metal transitions. Accordingly, metals are characterised by a low resistivity ($10^{-2} - 10^{-6} \Omega\text{cm}$) at room temperature, and as the temperature increases, the resistivity increases linearly. Semiconductors and insulators have higher and large ranging resistivities ($10^3 - 10^{17} \Omega\text{cm}$) at room temperature, which decreases exponentially with rising temperature [22].

Several vanadium oxides display thermochromic properties. These materials are exploited in several technological applications, such as electrical and optical switching devices along with several others that are discussed later in this review. The solid-state physics of vanadium oxides is focused around metal-insulator transitions and phase transitions as a function of temperature. These thermochromic materials display extraordinary electronic, structural, and magnetic behaviour and are still a matter of some debate with respect to theoretical remarks, particularly VO_2 and V_2O_3 [26,27,28,29,30].

2.1. V_2O_3

At room temperature, vanadium sesquioxide, V_2O_3 has the corundum structure with rhombohedral symmetry (**Fig. 3**). The vanadium ions are arranged in V-V pairs along the c

axis, perpendicular to the ‘honeycomb-like’ or distorted hexagonal lattice in the ab basal plane of metal ions, where only two of the three successive intersections are occupied by V^{3+} ions. Each V^{3+} ($3d^2$) ion is surrounded by O^{2-} ions, forming a distorted octahedron around each cation.

Direct information about the electronic structure of V_2O_3 has been obtained by photoemission and x-ray absorption spectroscopic studies since the 1970s. In addition, there have been a multitude of computational based studies that include dynamical mean field theory (DMFT), alongside standard density functional based methods, such as, local density approximation (LDA), which enable the calculation of spectral properties of materials with strong electronic Coulomb interactions. However, the electronic structure and the controversial nature of the magnetic properties of V_2O_3 continue to be a topic of interest [32].

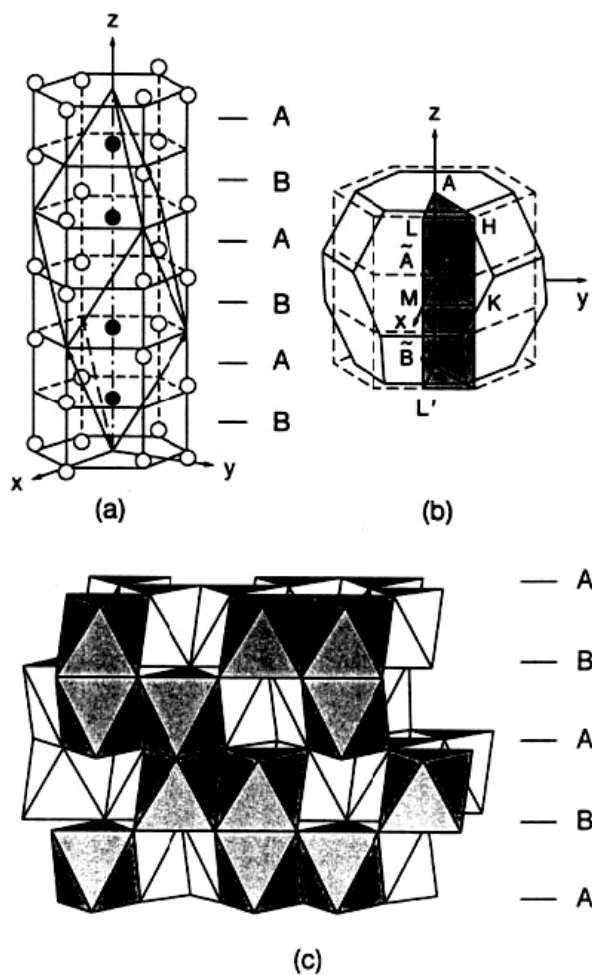


Fig. 3. (a) Vanadium-atom positions for corundum-phase V_2O_3 in the primitive rhombohedral (filled circles) and non-primitive hexagonal (circles) cells; (b) rhombohedral Brillouin zone (solid lines) and an equivalent hexagonal-type irreducible wedge; (c) the corundum structure as a linked network of face-sharing VO_6 octahedra with ordered vacancies (derived from NiAs with a vacancy at $1/3$ cation sites), reducing the space group symmetry from $P6_3/mmc$ to $R\bar{3}c$ [31].

V_2O_3 was discovered by Foex [33] in 1946, and is considered to be the prime example of a strongly correlated electron system that undergoes a Mott–Hubbard

transition. More recently, the concept of 3d-ligand orbital hybridization and charge transfer systems has been considered more appropriate, since the hybridization between V 3d and O 2p orbitals may change significantly across the phase transitions, so the single Hubbard band model may not hold. Consequently, it is often postulated that the semiconductor-to-metal transition mechanism may be intermediate between the Mott–Hubbard and charge-transfer models [34, 35].

The first order semiconductor-to-metal transition occurs at $T \approx 150K$ ($-123^\circ C$), from a low temperature antiferromagnetic monoclinic phase to a rhombohedral paramagnetic metallic phase [36]. The monoclinic distortion may be regarded as a shifting of the cation pairs in the corundum basal plane towards another, effectively tilting the c -axis [37]. The V–V distance along the hexagonal c axis is larger in the monoclinic insulating phase than in the rhombohedral metallic phase, and the significance of this bond is still a matter of some debate [38]. Nevertheless, there is general consensus that the single-band Hubbard model insufficiently describes the semiconductor-to-metal transition in V_2O_3 due to its complex multi-orbital nature [39].

2.2. V_2O_5

Vanadium pentoxide, V_2O_5 , has been found to exhibit thermochromic behaviour and undergoes a semiconductor-to-metal phase transition at 530 K ($257^\circ C$) [40]. Moreover, since its optical and electrical properties are associated, vanadium pentoxide also possesses electrochromic properties, displaying colour changes from blue to green and to yellow in a time period of approximately two seconds [41]. Electrochromic materials are characterized by their ability to sustain reversible and persistent changes of their optical properties in response to an applied voltage. The phenomenon of electrochromism therefore offers a relatively simple means of producing variable light transmission via electrochemical reactions [42].

The structure of V_2O_5 was determined by Bachmann (1961) [43]. Below the transition temperature in the semiconductor state, the band gap energy is ~ 2.24 eV and the structure is orthorhombic, composed of corner- and edge-sharing VO_6 octahedra (analogous to all other electrochromic metal oxides). The arrangement of the octahedra are, however, irregular since the V–O distances vary (Fig. 4) [44]. The orthorhombic structure has large V–O separations along the crystallographic c -axis, therefore the structure can be described in terms of layers of square pyramids of VO_5 (~ 0.44 nm apart), with five oxygen atoms surrounding the vanadium atom.

The layer structure of V_2O_5 (Fig. 5) makes it exceptionally well suited for the intercalation of cations, hence its application in thermally activated electrochromic devices.

The optical properties of the low temperature state have been well characterized, while the metallic state has been investigated very little [49].

2.3. VO_2

Vanadium (IV) oxide is by far the most studied solid-state thermochromic material. It shows great promise for

use in applications, such as “intelligent” architectural glazing. A single pure crystal of VO₂ has a semiconductor-to-metal transition temperature of 341 K (68 °C) [50]. There is a corresponding structural phase change upon passing T_c , from the low temperature monoclinic crystal structure to the high temperature rutile, tetragonal-type lattice [50, 51].

The high temperature rutile structure of metallic VO₂ is based on a simple tetragonal lattice (space group $P4_2/mnm$) (Fig. 6). The vanadium atoms are located at the equidistant Wyckoff positions (4f), (0, 0, 0) and $(\frac{1}{2}, \frac{1}{2}, \frac{1}{2})$ and each V atom is surrounded by an edge-sharing octahedron of oxygen atoms, VO₆, which occupy the positions at $\pm(u, u, 0)$ and $\pm(\frac{1}{2} + u, \frac{1}{2} - u, \frac{1}{2})$.

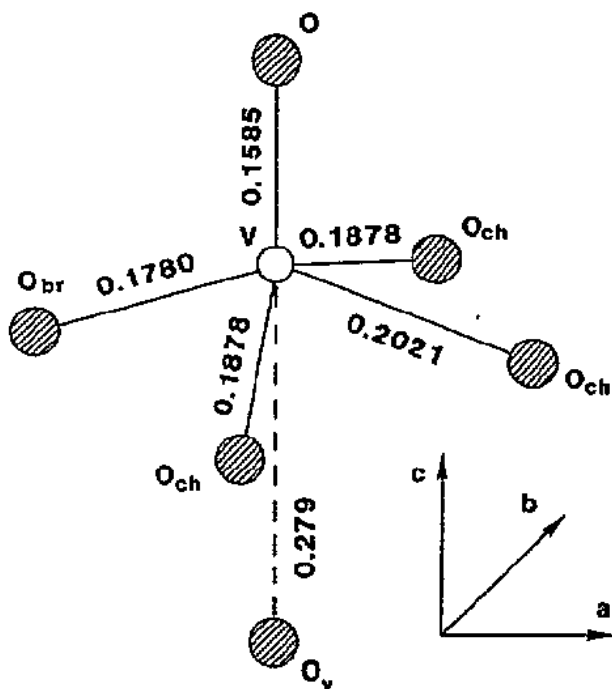


Fig. 4. The coordination of the vanadium ion in V₂O₅ [45] The V-O_{ch} bonds form puckered chains in the *b*-direction. These are linked by O_{br} bridging atoms in the *a*-direction. Layers are formed by the interaction of the weak V-O_v vanadyl bonds in the *c*-direction. The shorter bond length interactions are thought to be mainly covalent in nature, where as the long V-O interactions are considered to be more ionic [46].

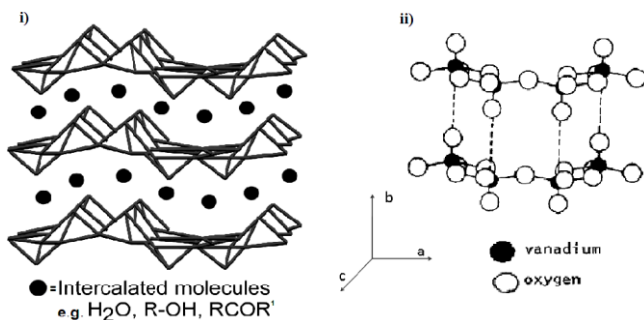


Fig. 5. i) Schematic of the orthorhombic crystal structure of V₂O₅, demonstrating the intercalation of molecules between the double layers of VO₅ square pyramids, resulting in its electrochromic properties [47]; ii) Illustration of the interactions between layers in orthorhombic V₂O₅ [48].

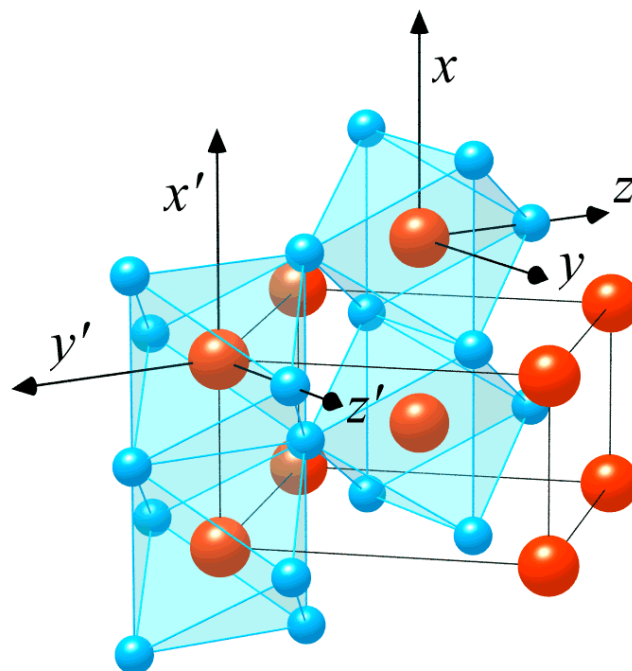


Fig. 6. The rutile structure of VO₂, when $T > T_c$. The large red circles represent V⁴⁺ ions, and the small blue circles are O²⁻ ions [52].

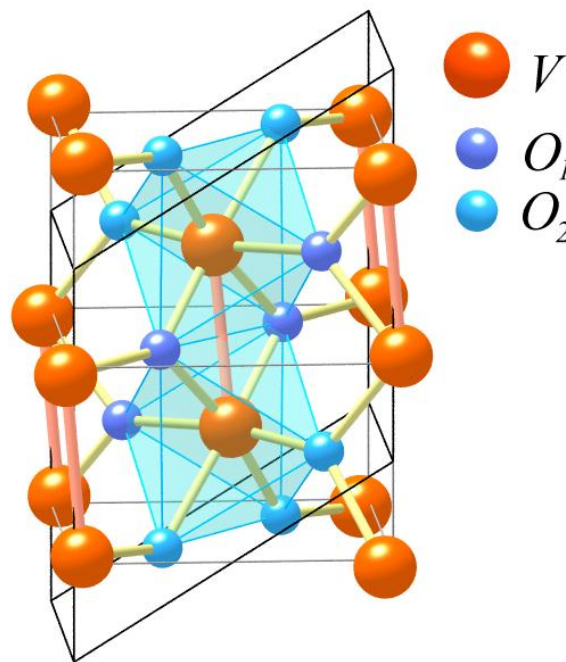


Fig. 7. The M₁ monoclinic structure of semiconducting VO₂ when $T < T_c$. Two types of oxygen ions can be distinguished [52].

The low temperature semiconducting phase of VO₂ belongs to the monoclinic crystal system (space group $P2_1/c$) (Fig. 7). At 25 °C the lattice has unit cell parameters; $a = 5.75 \text{ \AA}$, $b = 4.52 \text{ \AA}$, $c = 5.38 \text{ \AA}$ and $\beta = 122.60^\circ$. The lattice is the result of the distortion and doubling in size of the high temperature metallic tetragonal phase. The structure involves V⁴⁺-V⁴⁺ pairing with alternate shorter (0.265 nm) and longer (0.312 nm) V⁴⁺-V⁴⁺

distances along the monoclinic a axis, and tilting with respect to the rutile c -axis. The pure VO_2 phase is referred to as M_1 , since doping of vanadium (IV) oxide results in another monoclinic arrangement, M_2 (space group $C2/m$).

The nature of the semiconductor-to-metal transition in vanadium (IV) oxide has been investigated via computational, experimental and theoretical studies. The prime mechanism of the transition remains a mysterious phenomenon, since the three phases of VO_2 exhibit diverse lattice structures, but have analogous electronic properties, such as, the existence of the semiconductor-to-metal transition, similar activation energies and conductivities; the Mott-Hubbard model of correlating electrons were initially postulated [53].

Goodenough [50] (1971) proposed a useful explanation of the two phases of vanadium (IV) oxide, based on molecular orbitals and a band structure diagram (Fig. 8). An antiferroelectric transition was considered as the potential driving force for the semiconductor-to-metal transition in vanadium (IV) oxide. It was suggested that $\text{V}^{4+}\text{-V}^{4+}$ pairing in the tetragonal phase (Fig. 8a) becomes energetically stable after cooling, following rearrangement of the band structure to give the monoclinic phase (Fig. 8b). Subsequently, the onset of antiferroelectric and crystallographic distortion was found to occur at two different temperatures, but happen to be synchronized for vanadium (IV) oxide. Goodenough concluded that the antiferroelectric component of the monoclinic low temperature phase in VO_2 is the driving force of the distortion. Furthermore, the transition temperature, T_c is not controlled by thermal excitation of electrons into the anti-bonding bands, but by the entropy of the lattice vibrational modes.

Wentzcovitch *et al.* [55] (1994) reported convincing evidence from the results of LDA calculations, of the band-like character (Peierls insulator) of VO_2 to account for the low temperature monoclinic state, M_1 . These results were incorporated into Eyert's study that also used LDA calculations and a band theoretical approach, which elucidated the M_2 monoclinic phase of semiconducting VO_2 [52]. Cavalleri *et al.* [51] carried out experimental studies to endorse the band-like character using femtosecond laser excitation to initiate the transition and establish a time domain hierarchy. Subsequent measurements of the characteristic X-rays, optical signatures, transient conductivity and coherent phonons associated with between the structural and electronic effects in VO_2 thin films. The results indicated that the disappearance of the band gap was due to optical phonons that brought about the structural phase change. Thus, the atomic arrangement of the high-temperature rutile lattice was deemed to be essential for the occurrence of the metallic phase of VO_2 .

Upon passing through the transition temperature, the electrical conductivity increases significantly. This is accompanied by a dramatic increase in infrared reflectivity, with virtually no change in the visible region. Above T_c , the material reflects infrared radiation. Yet, below T_c , it is transparent, which is crucial in its application as a thin film coating for "intelligent" architectural glazing. An obvious problem for such application is the critical temperature of VO_2 being much too high at 68 °C (in comparison to room temperature), which can be rectified by using a dopant that

will lower the critical temperature. This is discussed later in this review.

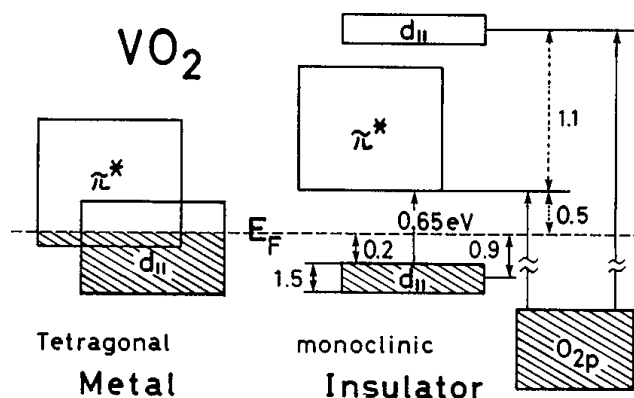


Fig. 8. Schematic band structure diagram of VO_2 [54]. The hybridisation of the V 3d and O 2p levels reflects the symmetries of the atomic arrangement in the crystal lattice.

2.4. V_6O_{13}

V_6O_{13} is a mixed-valence oxide with 4V^{4+} ($3d^1$) and 2V^{5+} ($3d^0$) and has a layered monoclinic crystal structure, similar to that of V_2O_5 . The composition of pure V_6O_{13} at room temperature is made of edge- and corner-sharing VO_6 octahedra, arranged in alternating single and double layers with corner sharing between the layers, in space group $C2/m$ (Fig. 9). There are three crystallographic non-equivalent vanadium atoms and seven non-equivalent oxygen atoms in the structure of V_6O_{13} [56].

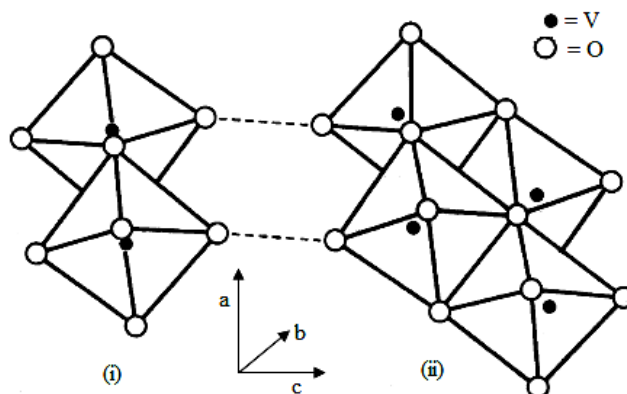


Fig. 9. The two distinguishable crystal structures in V_6O_{13} , simplified and adapted from [56] where i) the edge-sharing VO_6 octahedra form single zig-zag strings in the b -direction. The strings link together by corner-sharing to form single sheets parallel to the ab plane; and ii) the double zig-zag ribbons are formed by extending into the ac plane via edge-sharing VO_6 octahedra.

The three-dimensional lattice is formed by extensive edge-sharing of the VO_6 octahedra to form single and double ribbons, and common corner-sharing between single and double sheets.

There have been restricted studies on V_6O_{13} , due to the complicated physical properties and the crystal structure, in contrast to V_2O_3 . V_6O_{13} has been reported to undergo a

semiconductor-to-metal phase transition $T_c = 150$ K (-123 °C) and an antiferromagnetic transition at $T_c = 55$ K (-218 °C) [57]. This low-temperature structure was initially elucidated by Dernier [58] (1974) in the non-centrosymmetric space group C2, and later by Kawada *et al.* [59] (1978) in the centrosymmetric space group P21/a.

The nature of the semiconductor-to-metal transition is considered to be similar to that of V_2O_3 , although the complex band structure is not fully understood. It is suggested that the change in bandwidth for such mixed-valence vanadium-oxygen systems may be due to V-V pairing in the semiconducting phases or by a subsequent change in V-O distance [54].

V_6O_{13} is a transition-metal oxide that has been studied to a large extent as a potential cathode material for a lithium-polymer battery (with an associated metallic lithium anode). During the fully reversible insertion/discharge (lithiation) process, V_6O_{13} passes through a succession of phase transitions, and hosts as many as six Li atoms per V_6O_{13} unit [60].

2.5. Ti_nO_{2n+1} magnéli phases

Ti_2O_3 and Ti_3O_5 are members of the Magnéli series of Ti_nO_{2n+1} phases. Ti_2O_3 is isostructural with vanadium

sesquioxide, V_2O_3 , and possesses the corundum structure (Figure 3). However, the semiconductor-to-metal transition, as initially observed by Morin [17] (1959), differs from that observed in the vanadium oxide systems (first-order transition) given that the transition is ‘gradual’ (second-order transition) rather than ‘sharp’ (Fig. 1). The critical temperature therefore extends over a relatively broad (~ 250 K) range; between 450 K-600 K (127 - 377 °C) [22,61,62]. Unlike V_2O_3 , Ti_2O_3 does not undergo a simultaneous structural phase transition or change in symmetry, however the $Ti^{3+}-Ti^{3+}$ bonds of Ti^{3+} ion pairs become shorter as temperature decreases [63]. The origin and nature of the transition in Ti_2O_3 continues to be quarrelsome, however the results of early neutron spin-flip scattering experiments have discarded mechanisms based on magnetic-ordering phenomena. The current generally accepted opinion is that the metal-to-non-metal transition in rhombohedral Ti_2O_3 is caused by an uncharacteristic decrease in the c/a ratio with temperature, shifting the crucial energy-band states near to the Fermi level. This results in a small (~ 0.1 eV) semiconductor gap [61] arising between previously overlapping sub-bands of the Ti 3d manifold [64]. It is the general consensus that the transition in Ti_2O_3 cannot be explained in terms of a one-electron band picture,

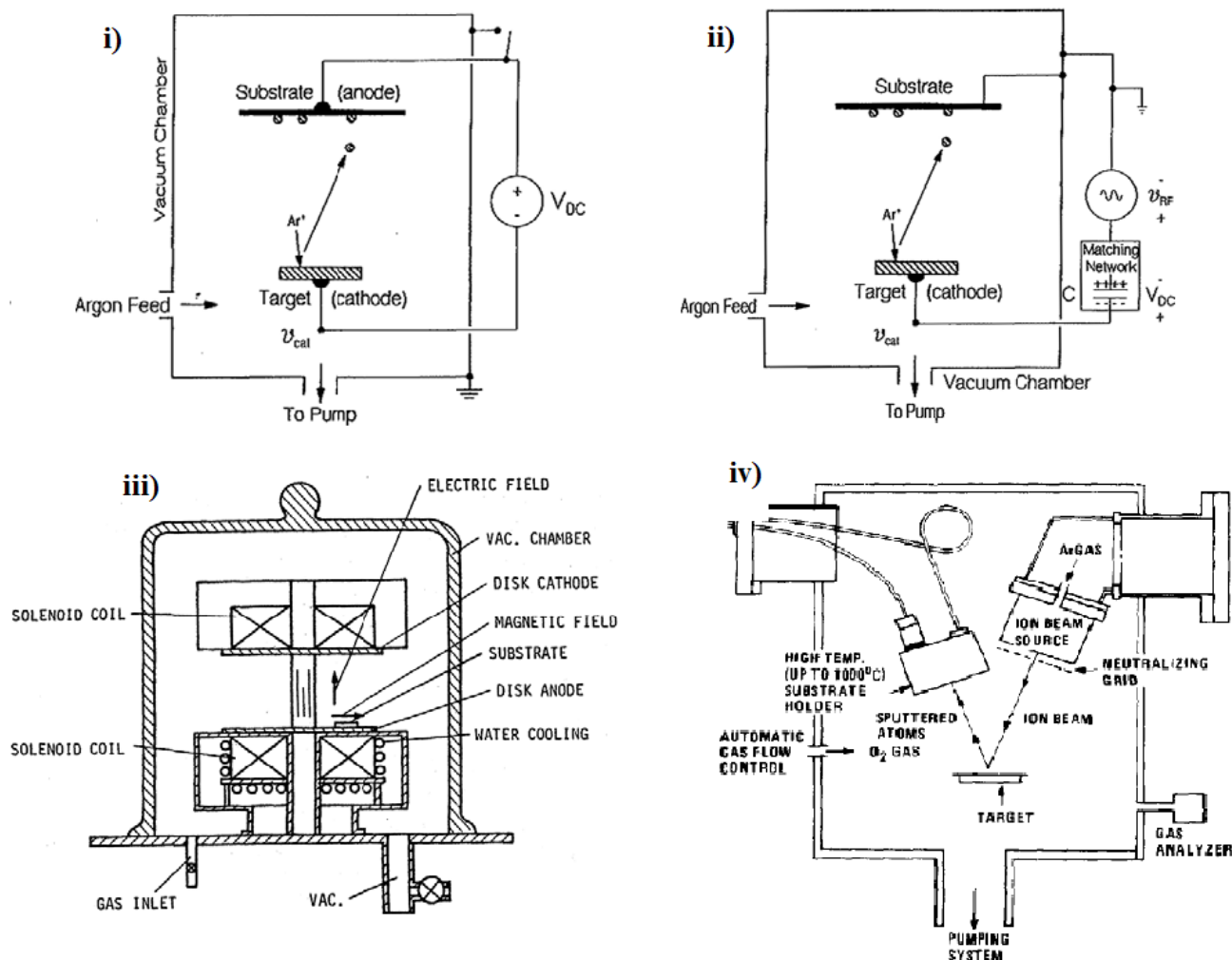


Fig. 10. PVD set-up from paper by Thornton (1983) [92], with (i) DC sputtering apparatus; (ii) RF sputtering apparatus; (iii) magnetron sputtering apparatus; (iv) ion beam sputtering system from paper by Jorgeson & Lee (1986) [90].

suggesting that consideration of electron correlation effects or the presence of intrinsic defects (titanium ‘interstitials’) may be required to explain the phenomenon. [62,65]

Ti₃O₅ occurs at room temperature as an insulator with a monoclinic structure (β -Ti₃O₅), and undergoes a phase transition at 177 °C to a second monoclinic structure (β') with an increase in cell volume [66]. Additional heating to 227 °C leads to a second phase transition and the formation of orthorhombic α -Ti₃O₅ [67]. The volume increase and phase transition at 177 °C are associated with an insulator metal transition. In the low temperature β phase, the titanium d-electrons are localized within a metal – metal bond; above the transition temperature these become delocalized. Breaking the metal – metal bonds result in relaxation of the structure and an expansion of the unit cell. It has been found that the Fermi level can be reduced by substituting Ti⁴⁺ with cations of a lower charge and a lower temperature transition is observed [68-70]. It has also been demonstrated that a similar effect can be observed using anionic substitution [71].

3. Effects of dopants

Amongst all of the thermochromic transition metal oxides discussed, vanadium (IV) oxide is the closest to room temperature, with its critical temperature, T_c at 68 °C. This is too high to be effective in many applications. For example the ideal transition temperature for “intelligent” glazing is in the region of 18-25 °C. Dopants can be incorporated into VO₂ to increase or decrease the thermochromic switching temperature, in order to make the VO₂ more commercially viable [72].

The way in which the introduction of dopants into the VO₂ lattice affects the temperature of the phase transition is, in fact, less understood than the nature of the semiconductor-to-metal transition itself. A comprehensive and elaborate discussion using analysis via X-ray diffraction is given by Goodenough in 1971 [50], who considered the presence of another semiconducting phase at high temperatures above T_c , existing between the monoclinic and tetragonal phase. This phase has an orthorhombic crystal structure for low-valence dopant ions and forms the rutile configuration for high-valence dopant ions.

Even though tungsten (VI) has been shown to reduce the thermochromic switching temperature of VO₂ by the greatest extent per atom %, there are a number of other dopants that can be incorporated into vanadium (IV) oxide. Dopant ion size and charge, and electron carrier density are factors that have been determined to affect T_c of vanadium (IV) oxide. Dopants with an atomic radii that is larger than the V⁴⁺ ion, or that create V⁵⁺ defects in the lattice, cause a decrease in T_c to around 25 °C, for example, the high valence metal ions tungsten (VI), niobium (V) and titanium (IV) [73]. Whereas, those with smaller ionic radii increase T_c such as, the low valence metal ions aluminium (III) and chromium (III) [73]. Although, changes in the critical temperature are only evident when large concentrations of the dopants are incorporated into the crystal structure [74]. A 2atm.% loading of tungsten proves to be the most effective dopant for reducing the critical temperature to

approximately 25 °C, when films are prepared by physical vapour deposition [75] and sol-gel coating [76]. A charge-transfer mechanism takes place, since a tungsten (VI) ion replaces a vanadium (IV) ion. The mechanism is postulated to be either via insertion of extra electrons into the vanadium *d*-band [77], as well as the larger ionic radius of tungsten over vanadium.

Sol-gel synthesis of VO₂ thin films can easily accommodate dopants and demonstrates a wide-ranging selection of dopant ions, since most of the first row transition metals having been employed [78]. Other dopants that have also been integrated into the VO₂ lattice by sol-gel methods, include gold [79] and molybdenum [80]. Only a small amount of gold (0.25 atom%) is required to decrease the transition temperature, however as the concentration of Au increases, the high temperature rutile phase of the doped VO₂ becomes less far infrared reflecting. Molybdenum has been found to lower T_c to 24 °C at a 7 atom % loading. Co-doping of molybdenum and tungsten, or tungsten and titanium into the VO₂ lattice works to afford very low thermochromic transition temperatures [81]. PVD techniques for producing doped-VO₂ thin films have not been as extensively studied and the range of metal ions that have been incorporated into the VO₂ lattice is not as ample as those investigated with sol-gel. Additionally, those that are known to induce the largest decrease in the semiconductor-to-metal transition temperature are the most studied. i.e. tungsten [75,77] and molybdenum [82, 83]. Fluorine has also been shown to reduce the transition temperature to 20 °C, whereby the fluorine atoms replacing oxygen atoms during doping, with 1.2 atom% fluorine. However, the hysteresis width of the thermochromic transition becomes substantially wider; hence fluorine doping is less appropriate for use in applications such as thermochromic window coatings.

The co-doping of tungsten and fluorine (in the range of up to 3 atom.% for both F and W) into VO₂ thin films by PVD is found to improve visible transmittance greater than tungsten-doped vanadium (IV) oxide, whilst reducing thermochromic transition temperature to around 27 °C [84].

4. Synthetic techniques

A variety of methods of depositing thermochromic thin films, especially vanadium (IV) oxide thin films, have been used, their basic operation and results are outlined below.

4.1 Physical vapour deposition

The physical vapour deposition (PVD) technique involves four steps including evaporation, transportation, reactions, and deposition. The material to be deposited, known as the target, is usually a solid-state metal precursor, which is bombarded by a high-energy source (such as a beam of electrons or ions) under reduced pressure. Thus, the atoms on the surface of the metal target become displaced and vaporised. There have been several systems employed to energetically remove atoms from a metal target, and most have been used to prepare vanadium (IV) oxide thin films. Reactive sputtering is one of the most common PVD techniques, and thermochromic thin films have been synthesised using RF magnetron sputtering [85,86,87], DC magnetron sputtering [45,88,89] and ion beam sputtering

[90] (Fig. 10). RF magnetron sputtering uses non-conducting targets, whereas, DC magnetron sputtering deposits thin films from metallic i.e. conducting targets. Reactive sputtering of a metal in an inert gas, with a small amount of an active gas present, has been used extensively as a technique for forming metallic compounds, for example, transition metal compounds of V, Nb, Ta, Mo and W, which are otherwise difficult to achieve. VO_2 thin films were first grown by reactive sputtering in Fuls *et al.* [91] who synthesised the films by reactive ion-beam sputtering of a vanadium target in an argon–oxygen atmosphere. Therefore, the gaseous vanadium reacts with the oxygen gas in the deposition chamber to form a VO_2 thin film by condensing onto a substrate.

Sputtering offers several advantages, such as the ability to produce uniform films, scalability to larger substrates, and efficient deposition. Although there are, of course, various disadvantages with this method, for instance, it is an off-line process with slow growth rates, relatively poor film adhesion and requires expensive equipment. By controlling the amount of material removed from the target, and the volume of reactive gas present in the deposition chamber, the composition and thickness of the film can be accurately determined. Doping is also easily achieved by placing another target in the deposition chamber. The amount of doping can be easily controlled by the relative sizes of the targets. Also, RF sputtering apparatus operates at lower voltage and gas pressures, and higher deposition rates when compared to other forms of sputtering, whilst introducing the possibility of sputtering of an electrically insulating target [93].

Sputtering offers several advantages, such as the ability to produce uniform films, scalability to larger substrates, and efficient deposition. Although there are, of course, various disadvantages with this method, for instance, it is an off-line process with slow growth rates, relatively poor film adhesion and requires expensive equipment. By controlling the amount of material removed from the target, and the volume of reactive gas present in the deposition chamber, the composition and thickness of the film can be accurately determined. Doping is also easily achieved by placing another target in the deposition chamber. The amount of doping can be easily controlled by the relative sizes of the targets. Also, RF sputtering apparatus operates at lower voltage and gas pressures, and higher deposition rates when compared to other forms of sputtering, whilst introducing the possibility of sputtering of an electrically insulating target [93].

4.2. Pulsed laser deposition

Thermochromic thin films have also, more recently, been deposited using laser ablation. Pulsed laser deposition (PLD) is another physical vapour deposition technique, initially developed for the deposition of oxide superconductors in the late 1980s, and is ideal for metal oxide film growth and was first used for VO_2 deposition by Borek *et al.* [94] in 1993. In PLD (Fig. 11) a high power pulsed laser beam is used to energetically remove atoms from a metal target of desired composition, which is placed inside a vacuum chamber. This can be an ultra high vacuum, or can be carried out in the presence of a

background gas, commonly oxygen when depositing oxides. The metal oxide material that is vaporized from the target is then deposited as a thin film on a substrate. One of the major advantages of PLD is the possibility of maintaining the stoichiometry of the target in the deposited films, due to the high rate of ablation allowing all elements or compounds of the target to simultaneously evaporate. The laser source is situated outside the reaction chamber, thus the system is easy to manage. Additionally, the growth of epitaxial and highly adherent films with low substrate temperatures occurs due to the emission of energetic ions during laser–target–vapour interaction. PLD is a clean, versatile, cost-effective deposition technique. However, the drawbacks include limited sample size, hence the difficulty in controlling film thickness and uniformity, and the splashing of particulates on the film, resulting surface defects under thermal shock. Several methods have been employed to reduce splashing, such as the use of a mechanical particle filter, whereby a velocity selector filters off slow-moving particulates. Another method involves using a high-density target and smooth surface, or to polish the target surface before each cycle. Using relatively lower energy density or slower deposition rates can also avoid particulate formation [95].

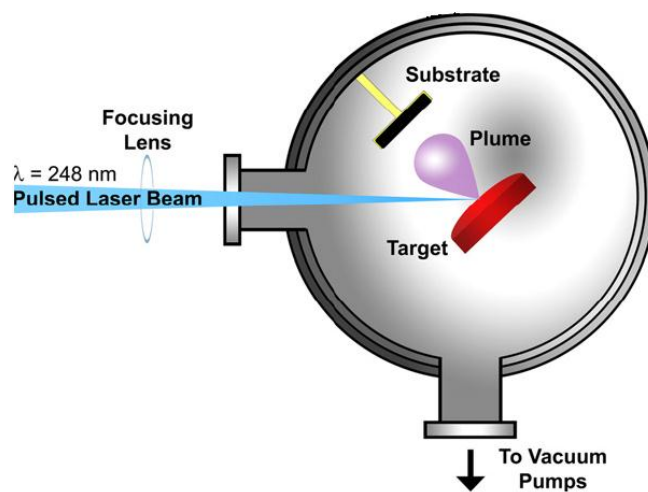


Fig. 11. A typical PLD. experimental arrangement. The laser beam is focused onto the target, which rotated to obtain uniform ablation [96].

Borek *et al.* ablated a metallic vanadium target with a KrF pulsed excimer laser (248 nm), in a deposition chamber with argon and 10% oxygen atmosphere of 100–200 mTorr, which was the oxygen partial pressure that favoured the deposition of pure VO_2 . Hence the oxygen to argon ratio was found to be a critical experimental parameter, since variations of partial O_2 pressures stabilize many different vanadium-oxygen phases that can subsist, for example V_2O_5 , V_3O_7 etc. The substrate temperature was maintained between 500 °C and 525 °C. Following the deposition, the samples were then annealed for approximately 1 h at the same temperature and pressure to obtain VO_2 films. In 1994 Kim *et al.* [97] reported that, using a KrF pulsed excimer laser (193 nm) on a target made of 99% pure pressed V_2O_3 powder, VO_2 thin films were grown on sapphire substrates, whilst maintaining the

temperature at 630 °C, after which the samples were cooled to room temperature without post-annealing, keeping the oxygen partial pressure constant. Room-temperature deposition of VO₂ by PLD without post-annealing has also been investigated, by Maaza *et al.* [98], and the as-deposited films exhibited sharp phase transitions at approximately 70 °C. However, room-temperature PLD of VO₂ thin films had not yet been achieved.

4.3. Sol-gel synthesis

Thin films production via the sol-gel method has been widely employed for depositing thermochromic VO₂ films [99, 100]. This synthesis route provides a relatively cheap and suitable method for large surface area deposition, with the ease of introducing metal dopants and relatively low processing temperatures. However, the films produced are of lower density than those deposited via PVD methods thus are more prone to cracking. The wet-chemical sol-gel technique is generally carried out by dip or spin coating various substrates into a chemical solution containing colloidal precursors (sol), typically metal alkoxide precursors which undergo hydrolysis and polycondensation reactions to form a colloid surrounded by solvent molecules. For example, the alkoxide is dissolved in an associated alcohol to form the sol, since different alcohols cause an assortment of transesterification reactions and the formation of various alkoxides. The sol is then treated with suitable drying (for porosity) and heating (for crystallinity) processes, to remove the solvent and encourage the formation of an inorganic network of a metal oxide. This involves connecting the metal centres with oxo (M–O–M) or hydroxo (M–OH–M) bridged polymers in a liquid phase (gel), which are then deposited onto the substrate. The preparation of VO₂ films generally begins with a dip- or spin-coated sol-gel V₂O₅ film and subsequent heat treatment in a vacuum or in a reducing atmosphere.

In 1983, Greenberg [101] introduced the ‘gelation-hydrolysis’ method for making crystalline VO₂, which involves partially hydrolysing the initial coating and subsequently annealing it in a reducing atmosphere. The most commonly used precursors for the sol-gel preparation of VO₂ films are vanadyl tri(iso-propoxide) and vanadyl tri(tert-amyloxy) [102]. Additional metal alkoxides or salts may be included in the precursor solution, in the required proportions, in order to readily introduce dopants into the network. The entire first row and many of the second and third row *d*-block elements have been doped into vanadium (IV) oxide using the sol-gel method.

In the 1990s, Livage *et al.* [103] found that vanadium dioxide and vanadium pentoxide gels can be synthesized via the acidification of aqueous solutions of vanadates, such as NaVO₃, or through the hydrolysis of vanadium oxo-alkoxides, for instance, VO(OR)₃ [73,76,104,105,106]. Yin *et al.* [107] demonstrated that V₂O₅ may be used as the precursor, instead of a vanadium alkoxide, which they claim offers advantages, such as the V₂O₅ precursor is cheap and easy to obtain, and the sol made by the quenching method they employed is stable.

The use of polyvanadate sols containing tungsten and molybdenum reported by Takahashi *et al.* [81,108], who dissolved metallic V, W and Mo powder in 30% hydrogen peroxide solution, which was then heated to form a hydrosol and spin coated onto a suitable substrate. The doped VO₂ film was then reduced in a hydrogen atmosphere.

4.4. Chemical vapour deposition

Chemical vapour deposition (CVD) is a standard industrial deposition process for the production of premium quality and highly functional thin films. The procedure differs from PVD, since a solid thin film results from a gaseous phase via chemical reactions on the heated substrate (Fig. 12).

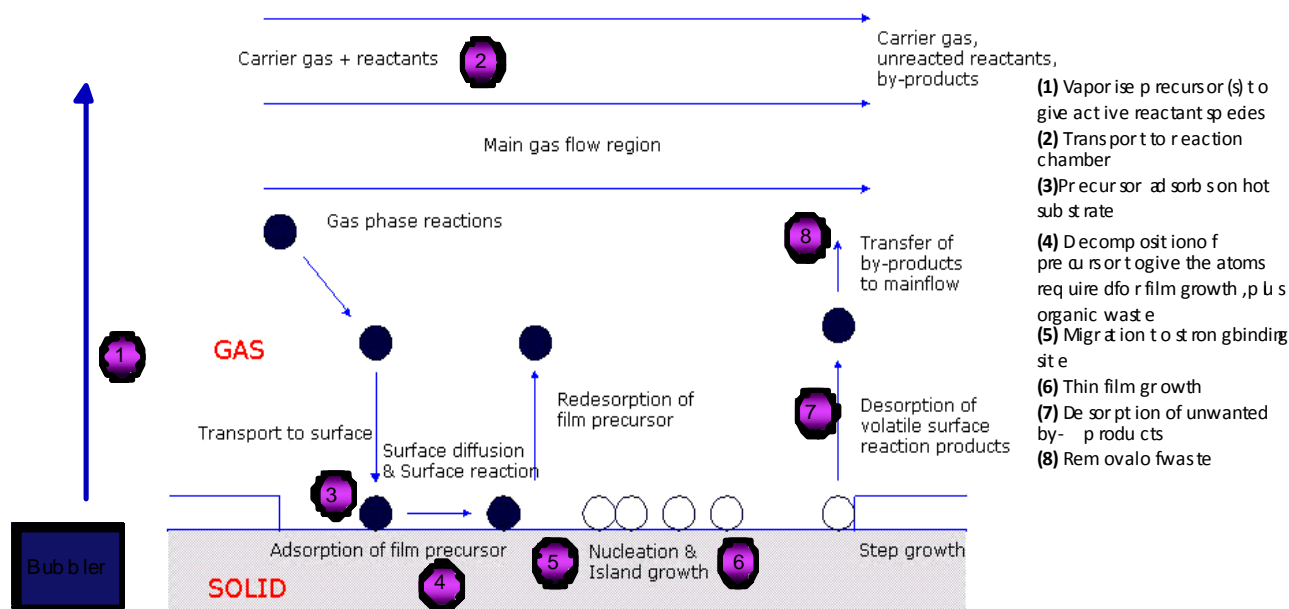


Fig. 12. Stepwise schematic diagram of the CVD process, including key for step 1-8, adapted from [109].

The main advantages of CVD are that the technique holds the ability to produce highly pure, dense materials and uniform films with excellent adhesion, high and adjustable deposition rates, at relatively low temperatures, and is reproducible. CVD is a non-line-of-sight process, so it can uniformly coat complex shaped substrates, thus depositing films with good conformal coverage; for example, low deposition rates favour the growth of epitaxial thin films for microelectronic components. High deposition rates tend to be used to deposit thick, protective coating. Process parameters are easily controlled and can be manipulated to determine the crystal structure, film orientation and morphology. There are a plethora of suitable chemical precursors for CVD, such as halides, hydrides, organometallics which enable the deposition of a large spectrum of materials including, metal, carbides, nitrides, oxides, sulphides etc. However, these precursors must be volatile. One of the shortcomings associated with CVD is the struggle to deposit multi-component materials with well-controlled stoichiometry, since different precursors have different vaporisation rates and it may therefore be unfavourable to use multi-source precursors, as opposed to the use of single-source precursors, which helps to eradicate this problem, but may lead to the incorporation of carbon impurities on the film surface [110].

The CVD process used for the production of vanadium (IV) oxide thin films is mainly based on the use of organometallic precursors, hence is frequently entitled metal-organic chemical vapour deposition (MOCVD) or organometallic chemical vapour deposition (OMCVD). Vanadium (V) oxide films are usually deposited and subsequent reduction results in the production of vanadium (IV) oxide thin films.

The first reported use of CVD for the deposition of VO_2 thin films was by Koide and Takei in 1966 [111]. They initially grew bulk single crystals of VO_2 by CVD. The following year they deposited thin films of VO_2 , using the same method with vanadium oxychloride (VOCl_3) precursors and N_2 carrier gas, which hydrolyzed onto the substrates producing epitaxial VO_2 films [112].

The next development occurred in the following year (1968) by MacChesney *et al.* [113], who exchanged the nitrogen carrier gas, with carbon dioxide, to transport the VOCl_3 precursor. Vanadium pentoxide, V_2O_5 formed on single-crystal sapphire substrates, which was then reduced to vanadium dioxide, VO_2 by annealing in a controlled atmosphere. This consisted of a mixture of CO and CO_2 gases at low oxygen partial pressures, between 500 °C and 550 °C.

Greenberg [101] was the first to successfully attempt CVD using vanadyl tri-isopropoxide, $\text{VO}(\text{OC}_3\text{H}_7)_3$ as a single source precursor in open atmosphere, with and without post-annealing. This resulted in pure VO_2 thin films coated onto glass substrates. Takahshi *et al.* [114] used vanadyl tri(isobutoxide) $\text{VO}(\text{O-i-Bu})_3$ as a single source precursor for depositing VO_2 thin films by dip-coating, as well as MOCVD at low pressure onto glass substrates, which resulted in discontinuous thin films with fine needle-like VO_2 crystals. Low-pressure CVD (LPCVD) has also been used to deposit thin films of VO_2 onto glass substrates [115, 116]. This work demonstrated that variations in the characteristics of the phase transition were a function of

film microstructure. The films were very dense at 475 °C and showed a large change in resistance at 66 °C, displaying a small temperature hysteresis in the transition. However, deposition at 520 °C led to films that exhibited a higher transition temperature of 72 °C, while the change in resistance was smaller with a larger hysteresis width. LPCVD is advantageous for window coatings since it is scalable to large substrates with good uniformity; however, a major drawback is the slow deposition rate.

In addition to organometallic precursors, vanadium halide precursors may be used, for example, VCl_4 or VOCl_3 , with water or ethanol as a source of oxygen [117,118], and the resultant films can then be reduced to vanadium(IV) oxide in an appropriate atmosphere. Furthermore Barreca *et al.* [119] used the CVD method with vanadyl precursors of general formula $\text{VO}(\text{L})_2(\text{H})$, where L is a β -diketonate ligand, at around 380 °C, in various atmospheres, such as O_2 , N_2 and a mixture of N_2 and H_2O , which resulted in VO_2 and V_2O_5 thin films. The precursors used in most of these studies are generally expensive and require post-deposition reduction to form the desired vanadium (IV) oxide thin films.

4.4.1. Atmospheric pressure chemical vapour deposition

Atmospheric pressure chemical vapour deposition (APCVD) is the most suitable method for high throughput deposition of thin films on glass substrates. In APCVD, the reaction chamber is approximately or precisely at atmospheric pressure. Consequently, in order to facilitate the transport of sufficient gaseous phase material to the reaction chamber, the precursors must have enough vapour pressure, therefore are required to be low-melting solids or volatile liquids. The reactants are transported to the reaction site via an inactive, hot carrier gas. The substrate temperature also needs to be relatively high to initiate the deposition. Two types of reaction may occur in the reaction chamber, either homogeneous reactions (occurs exclusively in the vapour phase) or heterogeneous reactions (occur at the vapour-solid surface interface). In cold-wall reactors homogeneous and heterogeneous reactions at the reactor walls are suppressed, hence vapour-substrate surface reactions prevail. The nature of these surface reactions is not fully understood, due to the difficulties in precisely determining the species at the reactive sites and the how the electronic structure of the solid surface determines the reaction kinetics.

APCVD takes advantage of comparatively simple apparatus, since no vacuum system is required, and other benefits include rapid growth rates and good conformal coverage of the entire substrate at low temperatures. The disadvantages of APCVD are poor thickness and step-coverage control, and potential film contamination. For example, the precursors VCl_4 and VOCl_3 may lead to the incorporation of the chlorine in the deposited film, or carbon contamination may occur from the use of a precursor such as $\text{V}(\text{acac})_3$.

There have been numerous studies of the growth of VO_2 thin films on glass or silica substrates. Maruyama and Ikuta [120] in 1993 used APCVD followed by post-deposition annealing, using vanadium (III) acetylacetonate, $\text{V}(\text{acac})_3$, as a single-source precursor to deposit

polycrystalline, pure VO₂ films on a substrate of fused quartz and sapphire single crystals. Manning *et al.* have extensively investigated APCVD of vanadium oxide thin films, and have successfully demonstrated doping of VO₂ with W, Ti, Mo, and Nb. They initially (2002) carried out APCVD using VCl₄ and water, to form thin films of V₂O₅, VO₂, VO_x ($x \approx 2.00\text{--}2.50$) and V₆O₁₃ on glass substrates at 400–550 °C [118]. Close control the deposition temperature of the reaction allowed the various vanadium oxide phases to be isolated. Higher temperatures encouraged the formation of oxygen poor phases. Also, the concentrations of the gaseous precursors in the reactions were also found to effect the phases deposited, where higher concentrations favoured the formation of oxygen rich vanadium oxides. VO₂ thin films were synthesised without requiring post-treatment reduction. In the following years (2004), VOCl₃ and H₂O (with an excess of water over VOCl₃) were used as dual source precursors for APCVD of thermochromic VO₂ thin films onto glass substrates, at reactor temperatures greater than 600 °C. A mixed phase of V₂O₅ and V₆O₁₃ were also produced in some small patches, which were reduced by controlling the flow rates through the reactor. V₂O₅ thin films were also prepared when the reactor temperatures were lowed below 600 °C, or where an excess of VOCl₃ over H₂O occurred [121]. Tungsten-doped films were also prepared using APCVD of vanadium(IV) chloride, tungsten(VI) ethoxide, and water at 500–600 °C, producing V_{0.99}W_{0.01}O₂ thin films on glass substrates [122]. The films displayed significantly reduced thermochromic switching temperatures, from 68 °C in bulk VO₂ to 42 °C, showing great promise for commercial use as a window coating in “intelligent” glazing. The same group has reported the growth of composite VO₂-TiO₂ thin films using the precursor combinations of VOCl₃, titanium (IV) chloride (TiCl₄) and water [123], and also with the combination of VOCl₃, titanium isopropoxide and water. These composite films exhibited photo-induced hydrophilicity with low contact angles, photocatalysis, and a reduced thermochromic switching temperature of 54 °C.

More recently, APCVD of vanadyl acetylacetonate, tungsten hexachloride in a 2% oxygen and 98% nitrogen atmosphere by Binions *et al.* [124] led to the production of tungsten doped or un-doped vanadium (IV) oxide films on glass substrates. Tungsten doping was found to decrease the transition temperature by 20 °C per 1% tungsten incorporated. The properties of the thermochromic transition were notably affected by the crystallographic orientation of the film, which is influenced by variations of growth rate. Along with film morphology, the film thickness was found to rule the extent of the transition and visible light transmittance through the film, but not the temperature at which the transition occurred. An evaluation of the literature available reveals that widely varying conditions have been investigated in terms of reactor types, flow rates, temperature ranges, and precursor concentrations.

4.4.2. Aerosol assisted chemical vapour deposition

Aerosol Assisted Chemical Vapour Deposition (AACVD) is where the precursor is dissolved into an appropriate solvent (i.e. it possesses the correct physical and chemical

properties to allow formation of the aerosol), followed by the ultrasonic generation of an aerosol. This is where the precursors are atomised into finely divided sub-micrometer liquid droplets. The aerosol droplets are then transported to the heated active deposition site via a flow of inert gas, generally N₂, and the solvent is evaporated or combusted to produce a solid thin film. One advantage of AACVD is that the precursor is not required to be volatile (as in APCVD) but must be soluble in the solvent. Hence, the use of unconventional precursors that were not previously functional with APCVD may be used, such as polyoxometallates or ionic powders [125,126]. Other advantages include the lower cost of the process, since the vapour precursor generation and delivery method is simplified, compared to the usual CVD method that uses a bubbler/vaporiser, and it can take place in an open environment without the requirement of a vacuum system or CVD chamber, when depositing oxide films. Additionally, AACVD often uses single-source precursors and it is often easier to control the precursor proportions in the solution than in the gas phase, hence multi-component materials are synthesised with relative ease and well controlled stoichiometry. Furthermore, rapid deposition can occur at moderately low temperatures owing to the small diffusion distances between reactant and intermediates. AACVD of thin films suffers from disadvantages such as adhesion of the film to the substrate may be at times weak, and gas phase reactions can take place, leading to film defects (e.g. pin holes due to the deposition of large particles), which can result in the production of powdery films.

Sahana *et al.* [127] (2002) used AACVD of vanadium (III) acetylacetonate [V(acac)₃] in a spray pyrolysis system with a controlled atmosphere to develop VO₂, V₂O₃ and V₂O₅ films, and vanadyl (IV) acetylacetonate, [VO(acac)₂], has been used to prepare the meta-stable rutile VO₂. This phase can be converted to the tetragonal structure by annealing in argon at 500 °C.

Picirillo *et al.* [128] deposited thin films of vanadium oxides on glass substrates using AACVD from V(acac)₃ and VO(acac)₂. The phase of vanadium oxide formed (V₂O₃, VO₂, or V₂O₅) was found to be determined by the varying experimental parameters, such as, the vanadium precursor, solvent, and carrier gas flow rate. Modification of the conditions allowed single-phase V₂O₃, VO₂, and V₂O₅ to be formed across whole substrates, and this study was the first to report the CVD synthesis of V₂O₃ thin films. The resultant films displayed interesting functional properties, including hydrophobicity (VO₂), heat mirror properties for solar control applications (V₂O₃), and hydrophilicity (V₂O₅). They then synthesised tungsten-doped VO₂ thin films via the same conditions as the previous used, i.e. ethanol and VO(acac)₂, and W(OC₂H₅)₅ was employed as the tungsten precursor. Various depositions were carried out using different tungsten concentrations to investigate the effect of the tungsten concentration on the thermochromic transition temperature, T_c [129]. It was found that monoclinic V_xW_{1-x}O₂ was the only phase present with a tungsten content of up to ~2% atom, where mixed phases, such as W–O or W–V did not form. There is a linear relationship between the amount of tungsten in the solution and the amount incorporated in the

films, demonstrating the potential of the AACVD methodology for the deposition of doped thin films. The undoped VO₂ sample deposited in the initial study using this methodology showed a transition temperature at roughly 58 °C, which is 10 °C lower than the value normally observed for VO₂ ($T_c = 68$ °C). The decrease is thought to be caused by a strain in the film, which is usually observed for films thinner than 300 nm [120]. They report that an amount of dopant of ~1% reduces the transition temperature of VO₂ by nearly 22 °C. Piccirillo *et al.* also produced niobium-doped vanadium dioxide ($V_xNb_{1-x}O_2$, $x = 0-0.037$) thin films were prepared by AACVD of vanadyl (IV) acetonate and niobium(V) ethoxide in ethanol [130]. The data indicated a good linear correlation between the value of T_c and niobium content in the film and that 2% niobium in the film lower the transition temperature by 15 °C. Although niobium is a less effective dopant than tungsten, to decrease the value of T_c , significant changes in the transmittance and reflectance properties of the films were observed; hence it is still considered a suitable material for application in intelligent architectural glazing.

Recently, hybrid CVD systems, the mixing of aerosol and atmospheric precursor flows, have been developed, boasting film characteristics similar to those produced by APCVD (i.e. good film adhesion, uniformity, and coverage) with the added versatility of the AACVD technique. For example, enhanced surface coverage was observed and an assortment of films of varying thickness and dopant levels were produced with reasonable ease. Binions *et al.* [131] (2008) produced thin films of gold nanoparticle-doped monoclinic vanadium (IV) oxide thin films via hybrid aerosol-assisted (AA) and atmospheric pressure (AP) CVD of vanadyl acetylacetonate and auric acid in methanol. They incorporated gold nanoparticles with strongly absorbing surface plasmon resonance (SPR) into VO₂ thin films. SPR is reversible and is stimulated thermally within the temperature range of 25-120 °C. The frequency of SPR (548 nm to 600 nm) is highly dependent on the dielectric properties of the host matrix, i.e. VO₂, and the size of the gold nanoparticles [98]. This research was implemented for the reason that, although tungsten has continually proved to be the most successful dopant for decreasing the transition temperature of VO₂, the major limitation on its commercial viability for exploitation in architectural glazing, is that tungsten-doped vanadium (IV) oxide thin films possess an unpleasant brown/yellow colour, which is retained upon thermochromic switching. Significant changes in the colour of the film, from the brown colour to a variety of greens and blues, can therefore be tuned by incorporation gold nanoparticles of the appropriate size and concentration. The use of auric acid as a single-source precursor for AACVD to produce gold nanoparticle films led to a wide nanoparticle size distribution [132]. Therefore, Binions *et al.* [133, 134] incorporated the use of a coordinating surfactant into the hybrid CVD synthesis for Au-doped VO₂ thin films, which controlled the size and shape of the deposited gold nanoparticles. The method was a one-step process that used a solution of preformed nanoparticles, VO(acac)₂ and tetraoctylammonium bromide (TOAB) in methanol. The TOAB was found not only to template the growth of gold nanoparticles doped into the film, but also the growth of the

film itself. Thus, additional strain was established in the films, which caused a reduction in the thermochromic transition temperature [135].

4.5. Comparison of production methods

The advantages and disadvantages of each synthetic technique for the deposition of solid-state thermochromic thin films were succinctly mentioned when discussing each method. Here, a summary and comparison of each procedure is presented.

Physical vapour deposition techniques require vacuum or reduced pressure conditions, which are time-consuming to achieve and maintain, and expensive evaporation/sputtering/ablation equipment, which increases production costs. Therefore, economic factors restrict the commercial applications of PVD. Moreover, the slow film growth rates associated with PVD methods make the system unsuitable for incorporation into modern float glass processes. However, this does allow for the more efficient use of precursors and aids the production of ultra thin films with relative ease, in comparison to CVD. PVD may operate at lower temperatures, hence is compatible with a variety of substrates. Given that no chemical reaction takes place in PVD, as opposed to CVD, careful precursor selection is not a major concern; however, the purity of the target is required to deposit non-contaminated thin films. What's more, a variety of targets can be incorporated into the system without difficulty, developing multilayer arrays [102].

PVD and sol-gel techniques are currently used by glass manufacturers for the production of coated-glass merchandise. These costly, off-line processes are nevertheless exorbitant when considering universal commercial exploitation. Sol-gel methods are straightforward to operate, but the time required to establish the sol is important for obtaining the desired product, thus can be a slow multi-step process. Full coverage of the substrate with moderately even thickness can be achieved (which can be tricky to control over a large substrate), by using readily available precursors, although these are often expensive. Dopants may be easily introduced and the sol-gel process has low processing temperatures. The process tends to have high levels of wastage, hence reducing efficiency and suitability for integrating into the industrial float-glass process. Additionally, sol-gel techniques frequently involve spin-coating the substrate, which is also difficult to achieve with very large areas of glass. Furthermore, it can be difficult to create multi-layer thin films via the use of sol-gel methodology [136].

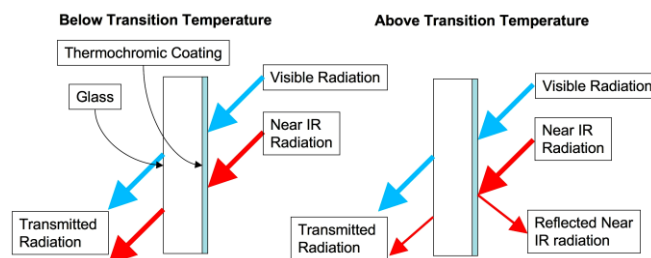


Fig. 13. Schematic representation of thermochromic materials applied as an intelligent window coating.

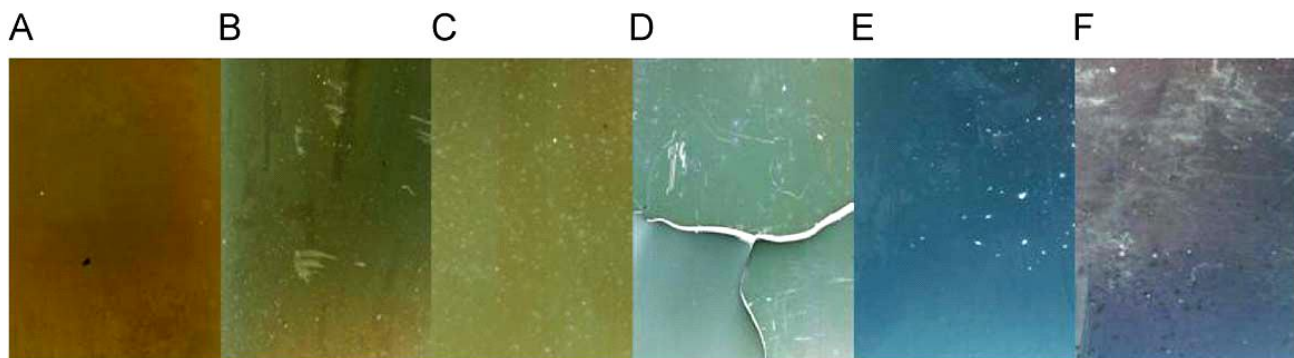


Fig. 14. Examples of glass ($3 \times 5 \text{ cm}^2$) approximate size with gold and vanadium dioxide nano composite films. The films had a Au/V ratio determined by EDAX of: (A) 0(W-doped VO_2), (B) 0.09, (C) 0.15, (D) 0.30, (E) 0.36 and (F) N (gold nanoparticle film) [135].

CVD is a non-line-of-sight process (unlike PVD) with high deposition rates at relatively low temperatures, thus depositing films with good conformal coverage and enables the synthesis of pure, dense and uniform thin films, which generally exhibit good adhesion. CVD is used extensively in the glazing industry, since it can easily be adapted into a float glass line. Ideally, a process that exploits readily available, low-cost precursors is required for an economical means of producing thermochromic products. Atmospheric pressure CVD is an ideal high-throughput method for producing thin films on glass substrates, because the equipment can be easily integrated into the float-glass production line, without the need of expensive vacuum systems, and the moderately high growth rates, compared to PVD. The precursors are often readily available and reasonably priced. APCVD methods are currently used by Pilkington-NSG for the production of K-glassTM and ActivTM [137].

5. Applications of thermochromic thin films

Solar control coatings can be applied to commercial or residential glazing, with the potential of improving the energy efficiency of buildings [138]. Vanadium (IV) oxide is an example of a thermochromic material that possesses the capability for use in intelligent window coatings, since its critical temperature ($T_c = 68 \text{ }^\circ\text{C}$) is closest to room temperature (Fig. 13).

The use of dopants to lower the thermochromic switching temperature has been extensively investigated, and tungsten (VI) is found to be the most promising. A major limitation of tungsten doping of VO_2 thin films in terms of commercial viability is the unattractive brown tint that the films possess when deposited on glass substrates (Fig. 14). Hence, the most recent work on VO_2 thin films by Binions *et al.* [135] focuses on improving the appearance of these potential window coatings, by incorporated gold nanoparticles as dopants. This not only reduces the transition temperature of VO_2 , but also gives the films a blue/green colour depending on gold concentration, which is must more appealing for consumers.

Energy modelling studies have been performed for the evaluation of the energy-saving characteristics of thermochromic glazing. The results suggest that thermochromic films may be useful in warmer climates but

are unsuitable for cooler climates, since the transition temperatures may be too high and the coating do not have sufficient time in the metallic state during the summer months (Fig. 15).

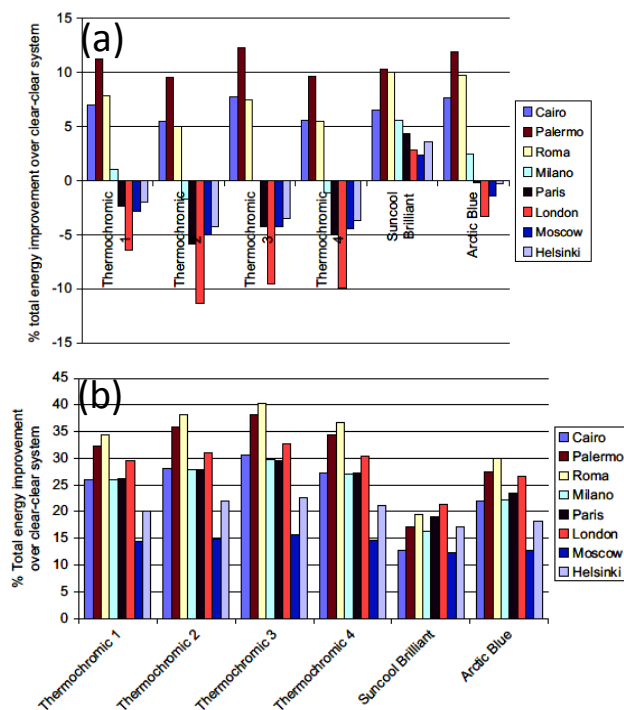


Fig. 15. Energy simulation results for (a) a residential scenario (25 % window), and (b) a commercial scenario (100 % glazing) with various window coatings [135].

Gold-doped vanadium (IV) oxide thin films have also received attention as fast optical switches [73,131]. Other potential applications of VO_2 thin films to exploit the ultra-fast switching could include solid-state devices, such as computational switches, optical mirrors and data storage or memory devices [139]. For example, Lee *et al.* [140] have demonstrated the application of VO_2 as a switching element in an oxide based memory with high speed and high density. This consists of a memory element (Pt/NiO/Pt) with non-volatile resistance switching behaviour, and a switching element (Pt/ VO_2 /Pt) with threshold resistance switching behaviour (Fig. 16). The main advantages for this type of memory assembly are the extremely rapid

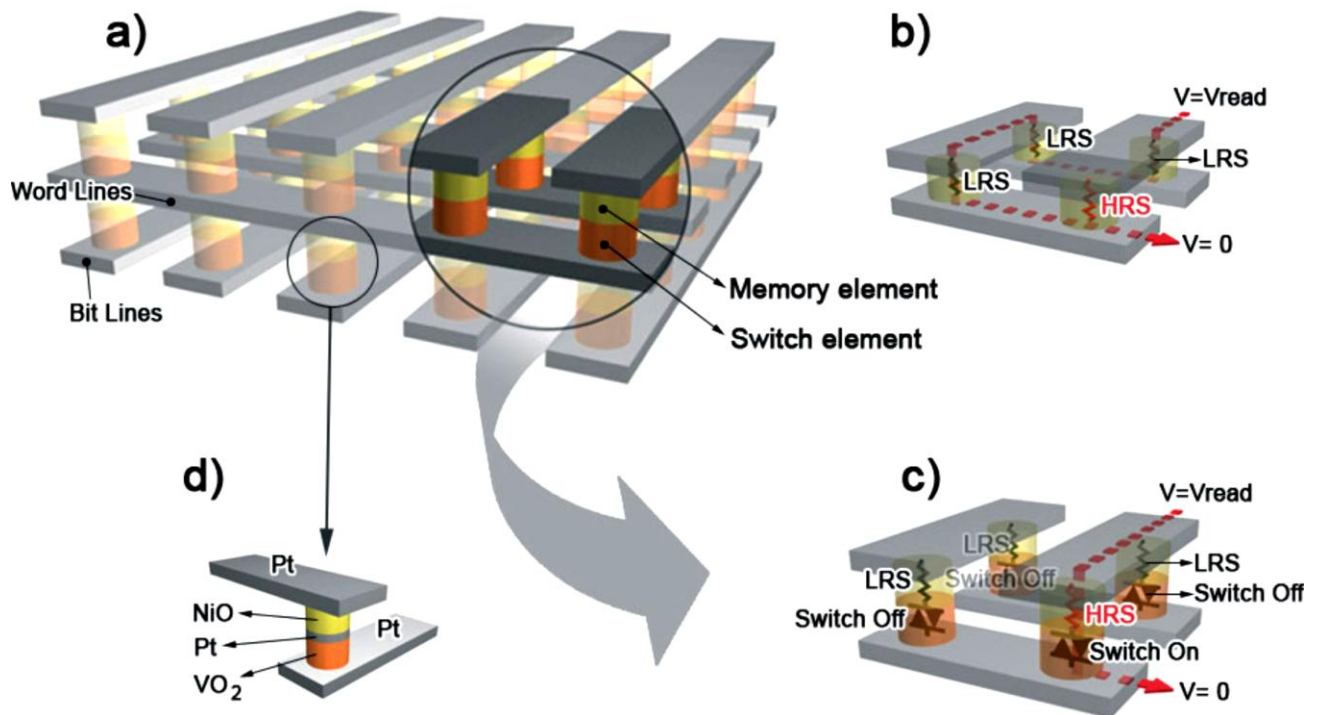


Fig. 16. a) Generalized cross bar memory structure whose one bit cell of the array consists of a memory element and a switch element between conductive lines on top (word line) and bottom (bit line). b) Reading interference in an array consisting of 2×2 cells without switch elements. c) Rectified reading operation in an array consisting of 2×2 cells with switch elements. d) Detailed structure of a single cell consisting of a Pt/NiO/Pt memory element and a Pt/VO₂/Pt switch element. SEM images of 30 nm Pt [140].

programming speed of several tens of nano-seconds, owing to the fast resistance switching characteristics and low processing temperature (below 300 °C) that are highly compatible with the 3-dimensional stack structures. These advantages indicate that non-volatile memory may favour the replacement of flash memory.

Vanadium pentoxide, V₂O₅, may have potential use in optical switches and write-erase media as well as vanadium (IV) oxide, since optical and electrical behaviour are coupled. V₂O₅ has also been suggested for use as a variable transmittance electrochromic device for controlling sunlight through windows [141].

6. Thermochromic lanthanide compounds

The lanthanum contraction, along the 4f rare earth series of the periodic table, produces profound effects with the progression of various transport and magnetic properties, when incorporated in perovskite nickelate materials [142]. Rare earth nickelate perovskites allow the relatively unambiguous study of the relationship between structural changes and physical properties. They were initially synthesized by Demazeau *et al.* [143] in 1971, and received a great deal of attention twenty years later due to the discovery of high-temperature superconductivity and giant

magnetoresistive effects in other perovskite-related systems. While the nickelates do not exhibit any of these characteristics, they are found to be one of the categories of oxides that demonstrate metallic conductivity. The existence of a very sharp metal–insulator transition in all the rare earth nickelates, with the exception of lanthanum nickelate (LaNiO₃), as was revealed by resistivity measurements [144, 145].

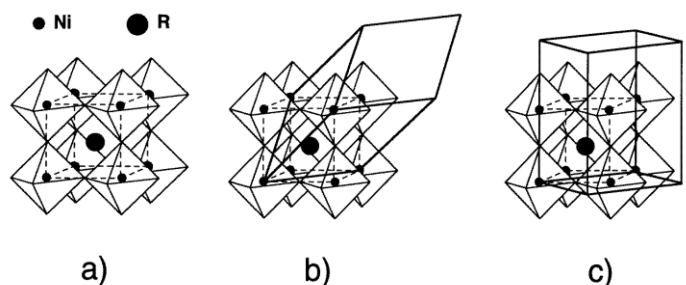


Fig. 17. a) The ideal perovskite structure (cubic $Pm\bar{3}m$); b) Rhombohedral distortion ($R3c$); c) Orthorhombic distortion ($Pbnm$) [142].

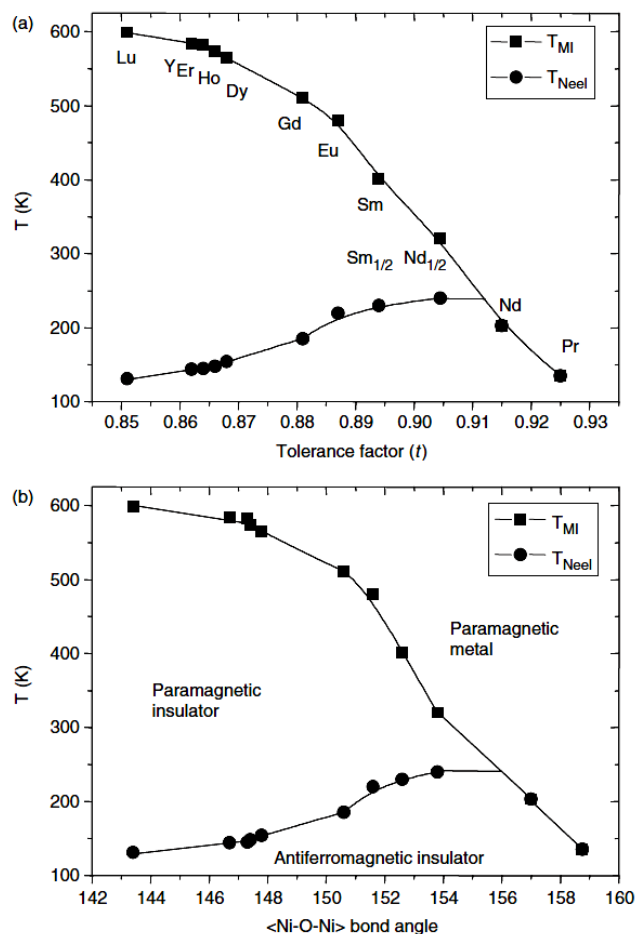


Fig. 18. Resistive and magnetic transitions as a function of (a) the tolerance factor t and (b) the Ni–O–Ni bond angle. The tolerance factor calculated using directly measured bond distances is smaller than that calculated using ideal ionic radii. This suggests that the bond in the nickelates is not purely ionic [146].

6.1. Rare earth nickelates

Rare earth nickelates are orthorhombically distorted perovskite oxides (space group $Pbnm$, of $GdFeO_3$ type) (Fig. 17) with the general formula $RNiO_3$, where R is a rare earth element, exhibit a metal–insulator transition temperature (T_{MI}) of 130 K (-140 °C), 200 K (-70 °C), 400 K (130 °C) and 560 K (290 °C) for $R = Pr, Nd, Sm$ and Gd , respectively. The transition temperature decreases with increasing size of the rare earth ion [144]. They display unusual magnetic order, charge order and, perhaps, orbital order, as well as sharp metal–insulator transitions. Furthermore, there are strong reasons to believe that some of them may be magnetoelectric multiferroics [146]. Below T_{MI} , in the insulating (semiconducting) phase, the perovskites are monoclinic (space group $P21/n$) and contain two chemically different Ni1 and Ni2 cations. This is thought to be a consequence of the charge disproportionation (CHD) of the Ni^{3+} ions, which is defined by the size difference between small and large NiO_6 . Upon heating across T_{MI} , the CHD vanishes and the two sets (Ni1 and Ni2) of three Ni–O bond lengths progressively increases to a maximum value, about 60–80 K below T_{MI} , and then suddenly vanishes at T_{MI} in the four compounds. An unexpected expansion of the b unit-cell parameter is

observed across the electronic phase transition, and a corresponding contraction is experienced by the a and c parameters. This Jahn-Teller effect is not reported for the earlier, lighter members of the series (Pr, Nd, Sm), and is the outcome of an extremely anisotropic rearrangement of Ni–O bond distances across the transition, in the ab basal plane.

7. Conclusion

Solid-state thermochromic materials undergo semiconductor-to-metal transition with an associated structural phase transitions at a critical temperature, T_c . Most of these materials possess unsuitably high or low thermochromic switching temperatures, and so their use in applications is limited. Vanadium (IV) oxide is the most studied thermochromic material due to its transition temperature being the closest to room temperature, and so exhibits the most potential for application in thermochromic devices. However, T_c of 68 °C is still too high, since applications such as intelligent thermochromic glass require switching temperatures between 18–25 °C. The precise switching temperature can be tuned by the level of doping, where tungsten (VI) is found to be the most promising. The challenges that must be overcome in order to manufacture a commercial window coating include factors such as colour, scale-up, and thermal cycling. Incorporating gold nanoparticles into the films via a hybrid aerosol-assisted and atmospheric pressure CVD technique shows potential to improve the colour of the VO_2 films, compared to the tungsten doped films, however, the cost of gold may prove to be an issue. The energy-saving performance of the films is predominantly controlled by the thermochromic switching temperature and number of hours the film spends in the hot state, rather than through the incorporation of gold nanoparticles. Simulation results show that, in warmer climates, a lower transition temperature leads to energy savings, thus reduction of the T_c to around room temperature will lead to further energy-saving behaviour. Au- VO_2 films also have the potential to be exploited in applications such as fast optical switches and memory devices. Rare earth nickelates have been shown to be a promising and potentially useful thermochromic material; although more research into them is required to realise this potential.

8. Acknowledgements

RB thanks the Royal Society for a Dorothy Hodgkin fellowship and the EPSRC for financial support (grant number EP/H005803/1).

9. Abbreviations

AACVD Aerosol assisted chemical vapour deposition, **APCVD** Atmospheric pressure chemical vapour deposition, **b** Lattice constant, **b_0** Critical value of lattice constant b , **CHD** Charge disproportionation, **CVD** Chemical vapour deposition, **DC** Direct current, **DMFT** Dynamical mean field theory, **G** Gibbs free energy, **k** Wavenumber quantum number, **LCAO** Linear combination of atomic orbitals, **LDA** Local density approximation, **LPCVD** Low-pressure chemical vapour deposition, **MOCVD** Metal-organic chemical vapour deposition, **OMCVD** Organometallic chemical vapour deposition, **P** Pressure, **PLD** Pulsed laser deposition, **PVD** Physical vapour deposition, **RF** Radio frequency, **SPR** Surface plasmon resonance, **T** Temperature, **T_c** Critical temperature, **TOAB**

Tetraoctylammonium bromide, ξ Landau order parameter, λ Wavelength.

10. References

- Mott, C. F. *Metal-insulator transitions*. 1974.
- Seredyuk, M.; Gaspar, A. B.; Ksenofontov, V.; Reiman, S.; Galyametdinov, Y.; Haase, W.; Rentschler, E.; Gütlich, P. **2006**, *18(10)*, 2513.
- Xie, H.; O'Dwyer, S.; Corish, J.; Morton-Blake, D. A. *Synthetic Metals* **2001**, *122(2)*, 287.
- Seeboth, A.; Klukowska, A.; Ruhmann, R.; Lötzsch, D. *Chinese Journal of Polymer Science* **2007**, *25(2)*, 123.
- Wilson, A. H. The Theory of Electronic Semi-Conductors. *Proceedings of the Royal Society of London. Series A* **1931**, *133(822)*, 458.
- Fowler, R. H. *Proc. R. Soc. London, Ser. A* **1933**, *140*, 505.
- Boer, J. H. d.; Verwey, E. J. W. *Proceedings of the Physical Society* **1937**, *49*, 59.
- Peierls, R. *Proc. Phys. Soc. London, Ser. A* **1937**, *49*, 72.
- Wigner, E. *Trans. Faraday Soc.* **1938**, *34*, 678.
- Mott, N. F. *Proceedings of the Physical Society. Section A* **1949**, *A69*, 416.
- Mott, *Reviews of Modern Physics* **1968**, *40(4)*, 677.
- Mott, N. F. *Phil. Mag.* **1961**, *6*, 287.
- Hubbard, J. *Proceedings of the Royal Society of London. Series A, Mathematical and Physical Sciences* **1964**, *281(1386)*, 401.
- Slater, J. C. *Phys. Rev.* **1951**, *82*, 538.
- Sparks, J. T.; Komoto, T. *Physics Letters A* **1967**, *25(5)*, 398.
- Brinkman, W. F.; Rice, T. M. *Physical Review B* **1970**, *2*, 4302.
- Morin, C. J. *Physical Review Letters* **1959**, *3(1)*, 34.
- Barker, C.A.S.C. *Physical Review Letters* **1966**, *17(26)*, 1286.
- Verleur, H. W.; Barker, A. S.; Berglund, C.N.O. *Reviews of Modern Physics* **1968**, *40*, 737.
- Abrahams, S. C. *Phys. Rev.* **1963**, *130*, 2230.
- Adler, D.; Brooks, H. *Physical Review* **1967**, *155*, 826.
- Adler, D. *Reviews of Modern Physics* **1968**, *40*, 714.
- Binder, K. *Reports on Progress in Physics* **1987**, *50(7)*, 783-859.
- Jones, H. *The Theory of Brillouin zones and electronic states in crystals*. Second, Revised edition ed., Amsterdam, North-Holland Pub. Co., **1975**.
- Kittel, C. *Introduction to Solid State Physics* 8th edn ed.; John Wiley and Sons.: New York, **2005**.
- Perucchi, A.; Baldassarre, L.; Postorino, P.; Lupi, S. *Journal of Physics: Condensed Matter* **2009**, *21(32)*, 323202.
- Held, K.; Keller, G.; Eyert, V.; Vollhardt, D.; Anisimov, V. I. *Physical Review Letters* **2001**, *86*, 5345.
- Imada, M.; Fujimori, A.; Tokura, Y. *Reviews of Modern Physics* **1998**, *70*, 039.
- Surnev, S.; Ramsey, M. G.; Netzer, F. P. *Progress in Surface Science* **2003**, *73(4-8)*, 117.
- Gupta, A.; Aggarwal, R.; Gupta, P.; Dutta, T.; Narayan, R. J.; Narayan, J. *Applied Physics Letters* **2009**, *95(11)*, 111915.
- Mattheiss, L. F. *Journal of Physics: Condensed Matter* **1994**, *6(32)*, 6477.
- Yethiraj, M., *Journal of Solid State Chemistry* **1990**, *88(1)*, 53.
- Foex, M. C. R. *Acad. Sci. III* **1946**, *223*, 1126.
- Zimmermann, R.; Claessen, R.; Reinert, F.; Steiner, P.; Hufner, S. *Journal of Physics: Condensed Matter* **1998**, *10(25)*, 5697.
- Pollini, I.; Mosser, A.; Parlebas, J. C. *Physics Reports* **2001**, *355(1)*, 1.
- Dernier, P. D.; Marizio, M. *Phys. Rev. B* **1970**, *2*, 3771.
- Adler, D.; Feinleib, J.; Brooks, H.; Paul, W. *Physical Review* **1967**, *155*, 851.
- Tanaka, A. *J. Phys. Soc. Jpn.* **2002**, *71*, 1091.
- Qazilbash, M. M.; Schafgans, A. A.; Burch, K. S.; Yun, S. J.; Chae, B. G.; Kim, B. J.; Kim, H. T.; Basov, D. N. *Physical Review B* **2008**, *77*, 15121.
- Nadkarni, G. S.; Shirodkar, V. S. *Thin Solid Films* **1983**, *105(2)*, 115.
- Shimizu, J.; Nagase, K.; Mirura, N.; Yamazoe, N. *Solid State Ionics* **1992**, *138*, L37.
- Granqvist, C. G. *Handbook of Inorganic Electrochromic Materials*, Elsevier, Amsterdam, **1995**.
- Bachmann, H. G.; Ahmed, F. R.; Barnes, W. H. *Z Kristallogr.* **1961**, *115*, 110.
- Talledo, A.; Granqvist, C. G. *Journal of Applied Physics* **1995**, *77(9)*, 4655.
- Talledo, A.; Granqvist, C. G. *Journal of Physics D: Applied Physics* **1994**, *27(11)*, 2445.
- Bachmann, H. G.; Barnes, W. H. *Z Kristallo-fr.* **1961**, *115*, 215.
- Whittaker, L.; Zhang, H.; Banerjee, S. *Journal of Materials Chemistry* **2009**, *19(19)*, 2968.
- Aldebert, P.; Baffier, N.; Gharbi, N.; Livage, J. *Materials Research Bulletin* **1981**, *16(6)*, 669.
- Chain, E. E. *Appl. Opt.* **1991**, *30(19)*, 2782.
- Goodenough, J. B. *Journal of Solid State Chemistry* **1971**, *3(4)*, 490.
- Cavalleri, A.; Dekorsy, T.; Chong, H. H. W.; Kieffer, J. C.; Schoenlein, R. W. *Physical Review. B Condensed Matter and Materials Physics* **2004**, *70(16)*, 161102.
- Eyert, V. The metal-insulator transitions of VO₂: A band theoretical approach, In *Annalen der Physik*, **2002**; pp 650-704.
- Zylbersztejn, A.; Mott, N. F. *Physical Review B* **1975**, *11*, 4383.
- Shin, S.; Suga, S.; Taniguchi, M.; Fujisawa, M.; Kanzaki, H.; Fujimori, A.; Daimon, H.; Ueda, Y.; Kosuge, K.; Kachi, S. *Physical Review B* **1990**, *41(8)*, 4993.
- Wentzcovitch, R. M.; Schulz, W. W.; Allen, P. B. *Physical Review Letters* **1994**, *72*, 3389.
- Wilhelmi, K. A.; Waltersson, K.; Kihlberg, L. *Acta Chem. Scand.* **1971**, *25*, 2675.
- Irizawa, A.; Higashiya, A.; Tsunekawa, M.; Sekiyama, A.; Imada, S.; Suga, S.; Yamauchi, T.; Ueda, Y.; Arita, M.; Takeda, Y.; Namatame, H.; Taniguchi, M.; Nanba, T. *Journal of Electron Spectroscopy and Related Phenomena* **2005**, *144-147*, 345.
- Dernier, P. D. *Materials Research Bulletin* **1974**, *9(7)*, 955.
- Kawada, I.; Ishii, M.; Saeki, M.; Kimizuka, N.; Nakano-Onoda, M.; Kato, K. *Acta Crystallographica Section B* **1978**, *34(3)*, 1037.
- Howing, J.; Gustafsson, T.; Thomas, J. O. *Acta Crystallographica Section B-Structural Science* **2003**, *59*, 747.
- Honig, J. M.; Zandt, L. L. V. *Annual Review of Materials Science* **1975**, *5(1)*, 225.
- Mattheiss, L. F. *Journal of Physics: Condensed Matter* **1996**, *8(33)*, 5987.
- Tanaka, A. *Physica B-Condensed Matter* **2004**, *351(3-4)*, 240.
- Honig, J. M. In *Nature of the Electrical Transition in Ti₂O₃*. **1968**, *40*, 748.
- Lucovsky, G.; Sladek, R. J.; Allen, J. W. *Physical Review B* **1977**, *16*, 5452.
- Salamat, A.; Hyett, G.; Cabrera, R. Q.; McMillan, P. F.; Parkin, I. P. *The Journal of Physical Chemistry C* **2010**, *114(18)*, 8546.
- Onoda, M. Phase Transitions of Ti₃O₅. *J. Solid State Chem.* **1998**, *136(1)*, 67.
- Grey, I. E.; Li, C.; Madsen, I. C. *J. Solid State Chem.* **1994**, *113(1)*, 62.
- Grey, I. E.; Ward, J. J. *Solid State Chem.* **1973**, *7(3)*, 300.
- Kellerman, D. G.; Zhilyaev, V. A.; Perelyaev, V. A.; Shveikin, G. P. *Inorganic Materials* **1983**, *19*, 221.
- Hyett, G.; Green, M. A.; Parkin, I. P. *Journal of the American Chemical Society* **2007**, *129*, (50), 15541.
- Pierce, J. W.; Goodenough, J. B. *Physical Review B* **1972**, *5(10)*, 4104.
- Béteille, F.; Livage, J. *Journal of Sol-Gel Science and Technology* **1998**, *13(1)*, 915.
- MacChesney, J. B.; Guggenheim, H. J. *J. Phys. Chem. Solids* **1969**, *30(2)*, 225.
- Burkhardt, W.; Christmann, T.; Meyer, B. K.; Niessner, W.; Schalch, D.; Scharmann, A. *Thin Solid Films* **1999**, *345(2)*, 229.
- Livage, J. *Coordination chemistry reviews* **1999**, *190-192*, 391.
- Jin, P.; Nakao, S.; Tanemura, S. *Thin Solid Films* **1998**, *324(1-2)*, 151.
- Lu, S.; Hou, L.; Gan, F. *Advanced Materials* **1997**, *9(3)*, 244.
- Cavanna, E.; Segaud, J. P.; Livage, J. *Materials Research Bulletin* **1999**, *34(2)*, 167.
- Hanlon, T. J.; Coath, J. A.; Richardson, M. A., *Thin Solid Films* **2003**, *436(2)*, 269.
- Takahashi, I.; Hibino, M.; Kudo, T. T. *Japanese Journal of Applied Physics* **2001**, *40(3A)*, 1391.
- Jin, P.; Tanemura, S. *Thin Solid Films* **1996**, *281-282(1-2)*, 239.
- Wu, Z. P.; Miyashita, A.; Yamamoto, S.; Abe, H.; Nashiyama, I.; Narumi, K.; Naramoto, H. *Journal of Applied Physics* **1999**, *86(9)*, 5311.

84. Burkhardt, W.; Christmann, T.; Franke, S.; Kriegseis, W.; Meister, D.; Meyer, B. K.; Niessner, W.; Schalch, D.; Scharmann, A. *Thin Solid Films* **2002**, 402(1-2), 226.
85. Xue-Jin, W.; et al. *Chinese Physics B* **2008**, 17(9), 3512.
86. Jin, P.; Tanemura, S. *Japanese Journal of Applied Physics, Part 1: Regular Papers and Short Notes and Review Papers* **1994**, 33(3A), 1478-1483.
87. Kana, J. B. K.; Ndjaka, J. M.; Ateba, P. O.; Ngom, B. D.; Manyala, N.; Nemraoui, O.; Beye, A. C.; Maaza, M. *Applied Surface Science* **2008**, 254(13), 3959.
88. Ghanashyam Krishna, M.; Debaugue, Y.; Bhattacharya, A. K. *Thin Solid Films* **1998**, 312(1-2), 116.
89. Sobhan, M. A.; Kivaisi, R. T.; Stjerna, B.; Granqvist, C. G. *Solar Energy Materials and Solar Cells* **1996**, 44(4), 451.
90. Jorgenson, G. V.; Lee, J. C. *Solar Energy Materials* **1986**, 14(3-5), 205.
91. Fuls, E. N.; Hensler, D. H.; Ross, A. R., *Applied Physics Letters* **1967**, 10(7), 199.
92. Thornton, J. A. *Thin Solid Films* **1983**, 107(1), 3.
93. Wasa, K.; Kitabatake, M.; H., A. *Thin film materials technology, Sputtering of compound materials* Springer, William Andrew Inc publishing, New York, **2004**.
94. Borek, M.; Qian, F.; Nagabushnam, V.; Singh, R. K. *Applied Physics Letters* **1993**, 63(24), 3288.
95. Jackson, T. J.; Palmer, S. B. *Journal of Physics D-Applied Physics* **1994**, 27(8), 1581.
96. Nag, J.; Jr, R. F. H. *Journal of Physics: Condensed Matter* **2008**, 20(26), 264016.
97. Kim, D. H.; Kwok, H. S. *Applied Physics Letters* **1994**, 65(25), 3188.
98. Maaza, M.; Bouziane, K.; Maritz, J.; McLachlan, D. S.; Swanepool, R.; Frigerio, J. M.; Every, M. *Optical Materials* **2000**, 15(1), 41.
99. Partlow, D. P.; Gurkovich, S. R.; Radford, K. C.; Denes, L. J. *Journal of Applied Physics* **1991**, 70(1), 443.
100. Lu, S.; Hou, L.; Gan, F. *Journal of Materials Science* **1993**, 28(8), 2169.
101. Greenberg, C. B. *Thin Solid Films* **1983**, 110(1), 73.
102. Parkin, C. P. *Journal of Nano Research* **2008**, 2, 1.
103. Livage, J. *Chemistry of Materials* **1991**, 3(4), 578.
104. Livage, J. *Solid State Ionics* **1996**, 86-88(Part 2), 935.
105. Livage, J.; Guzman, G.; Beteille, F.; Davidson, P. *Journal of Sol-Gel Science and Technology* **1997**, 8(1), 857.
106. Guzman, G.; Morineau, R.; Livage, J. *Materials Research Bulletin* **1994**, 29(5), 509.
107. Yin, D.; et al. *Journal of Physics D: Applied Physics* **1996**, 29(4), 1051.
108. Takahashi, I.; Hibino, M.; Kudo, T. *Japanese Journal of Applied Physics* **1996**, 35(4A), L438.
109. Pierson, H. O. *Handbook of Chemical Vapour Deposition*, William Andrew Publishing, New York, **1992**.
110. Choy, C. L. *Progress in Materials Science* **2003**, 48(2), 57.
111. Koide, S.; Takei, H. *J. Phys. Soc. Japan* **1966**, 21, 1010.
112. Koide, S.; Takei, H. *J. Phys. Soc. Japan* **1967**, 22, 946.
113. MacChesney, J. B.; Potter, J. F.; Guggenheim, H. J. *Journal of The Electrochemical Society* **1968**, 115(1), 52.
114. Takahashi, Y.; Kanamori, M.; Hashimoto, H.; Moritani, Y.; Masuda, Y. *Journal of Materials Science* **1989**, 24(1), 192.
115. Sahana, M. B.; Dharmaprakash, M. S.; Shivashankar, S. A. *Journal of Materials Chemistry* **2002**, 12(2), 333.
116. Sahana, M. B.; Shivashankar, S. A. *Journal of Materials Research* **2004**, 19(10), 2859.
117. Field, M. N.; Parkin, I. P. *A Journal of Materials Chemistry* **2000**, 10, (8), 1863.
118. Manning, T. D.; Parkin, I. P.; Clark, R. J. H.; Sheel, D.; Pemble, M. E.; Vernadou, D. *Journal of Materials Chemistry* **2002**, 12(10), 2936.
119. Barreca, D.; Depero, L. E.; Franzato, E.; Rizzi, G. A.; Sangaletti, L.; Tondello, E.; Vettori, U. *Journal of The Electrochemical Society* **1999**, 146(2), 551.
120. Maruyama, T.; Ikuta, Y. *Journal of Materials Science* **1993**, 28(18), 5073.
121. Manning, T. D.; Parkin, I. P. *Polyhedron* **2004**, 23(18), 3087.
122. Manning, T. D.; Parkin, I. P.; Pemble, M. E.; Sheel, D.; Vernadou, D. *Chemistry of Materials* **2004**, 16(4), 744.
123. Qureshi, U.; Manning, T. D.; Parkin, I. P. *Journal of Materials Chemistry* **2004**, 14(7), 1190.
124. Binions, R.; Hyett, G.; Piccirillo, C.; Parkin, I. P. *Journal of Materials Chemistry* **2007**, 17(44), 4652.
125. Cross, W. B.; Parkin, I. P. *Chemical Communications* **2003**, 14, 1696.
126. Binions, R.; Carmalt, C. J.; Parkin, I. P. *Thin Solid Films* **2004**, 469-470, 416.
127. Sahana, M. B.; Subbanna, G. N.; Shivashankar, S. A. *Journal of Applied Physics* **2002**, 92(11), 6495.
128. Piccirillo, C.; Binions, R.; Parkin, I. P. *Chemical Vapor Deposition* **2007**, 13(4), 145.
129. Piccirillo, C.; Binions, R.; Parkin, I. P. *Thin Solid Films* **2008**, 516(8), 1992.
130. Piccirillo, C.; Binions, R.; Parkin, I. P. *European Journal of Inorganic Chemistry* **2007**, 25, 4050.
131. Binions, R.; Piccirillo, C.; Palgrave, R. G.; Parkin, I. P. *Chemical Vapor Deposition* **2008**, 14(1-2), 33.
132. Palgrave, R. G.; Parkin, I. P. *Journal of the American Chemical Society* **2006**, 128(5), 1587.
133. Saeli, M.; Binions, R.; Piccirillo, C.; Hyett, G.; Parkin, I. P., *Polyhedron* **2009**, 28(11), 2233.
134. Saeli, M.; Binions, R.; Piccirillo, C.; Parkin, I. P. *Applied Surface Science* **2009**, 255(16), 7291.
135. Saeli, M.; Piccirillo, C.; Parkin, I. P.; Ridley, I.; Binions, R., *Solar Energy Materials and Solar Cells* **2010**, 94, (2), 141-151.
136. Kanu, S. S.; Binions, R. *Proceedings of the Royal Society A: Mathematical, Physical and Engineering Science* **2010**, 466(2113), 19.
137. Binions, R.; Carmalt, C. J.; Parkin, I. P. *Measurement Science & Technology* **2007**, 18(1), 190.
138. Granqvist, C. G. *Thin Solid Films* **1990**, 193-194(Part 2), 730.
139. Ruzmetov, D.; Ramanathan, S., In *Metal-Insulator Transition in Thin Film Vanadium Dioxide*, **2010**, pp 51-94.
140. Lee, M.-J.; Park, Y.; Suh, D.-S.; Lee, E.-H.; Seo, S.; Kim, D.-C.; Jung, R.; Kang, B.-S.; Ahn, S.-E.; Lee, C. B.; Seo, D. H.; Cha, Y.-K.; Yoo, I.-K.; Kim, J.-S.; Park, B. H. *Advanced Materials* **2007**, 19(22), 3919.
141. Cogan, S. F.; Nguyen, N. M.; Perrotti, S. J.; Rauh, R. D. *Proc.Soc. Photo-Opt. Instrum. Eng.* **1988**, 57, 1016.
142. Medarde, M. L. *Journal of Physics: Condensed Matter* **1997**, 9(8), 1679.
143. Demazeau, G.; Marbeuf, A.; Pouchard, M.; Hagenmuller, P. *J. Solid State Chem* **1971**, 3, 582.
144. Lacorre, P.; Torrance, J. B.; Pannetier, J.; Nazzal, A. I.; Wang, P. W.; Huang, T. C. *Journal of Solid State Chemistry* **1991**, 91(2), 225-237.
145. Torrance, J. B.; Lacorre, P.; Nazzal, A. I.; Ansaldo, E. J.; Niedermayer, C. *Physical Review B* **1992**, 45, 8209.
146. Catalan, G. *Phase Transitions: A Multinational Journal* **2008**, 81(7), 729.
147. Capon, *Journal of physics. D Applied physics* **2009**, 42, 18.
148. Napierala, C.; Edely, M.; Laffez, P.; Sauques, L. *Optical Materials* **2009**, 31, 1498.

Advanced Materials Letters

Publish your article in this journal

[ADVANCED MATERIALS Letters](#) is an international journal published quarterly. The journal is intended to provide top-quality peer-reviewed research papers in the fascinating field of materials science particularly in the area of structure, synthesis and processing, characterization, advanced-state properties, and applications of materials. All articles are indexed on various databases including [DOAJ](#) and are available for download for free. The manuscript management system is completely electronic and has fast and fair peer-review process. The journal includes review articles, research articles, notes, letter to editor and short communications.

